

Figure 3

Cardiac function by echocardiography in CXMD_j **A:** Sequential studies in echocardiographic parameters with advancing age in normal and CXMD_j dogs. LVIDd (mm), IVS and PW thickness (mm), and FS (%) in a normal littermate III-301MN (open circle), and the CXMD_j dogs III-302MA (closed circle) and III-303MA (closed square) at 2, 3, 4, 6, 9, 12, 15, 18, and 21 months of age. **B:** M-mode echocardiogram in a normal littermate III-301MN, compared to the CXMD_j dog III-302MA at 21 months of age. Hypokinesis of the left ventricular posterior wall was observed in the CXMD_j dog.

Table 2: Echocardiographic findings in normal and CXMD_J male dogs

| | Age (mo) | LVIDd (mm) | LVIDs (mm) | IVS (mm) | PW (mm) | FS (%) |
|-----------------------------|----------|------------|------------|----------|---------|--------|
| Normal male dogs | | | | | | |
| III-D56MN | 6 | 34.2 | 12.5 | 6.6 | 5.6 | 63.5 |
| III-1804MN | 7 | 30.7 | 18.9 | 8.2 | 7.4 | 38.4 |
| III-D03MN | 14 | 32.8 | 16.8 | 10.0 | 9.4 | 48.7 |
| III-301 MN | 21 | 36.1 | 23.0 | 7.0 | 6.4 | 36.2 |
| CXMD _J male dogs | | | | | | |
| III-D53MA | 6 | 29.7 | 19.7 | 8.0 | 7.2 | 33.8 |
| III-D55MA | 7 | 28.7 | 15.4 | 6.3 | 6.3 | 46.5 |
| III-1803MA | 7 | 32.5 | 16.7 | 5.8 | 7.5 | 48.5 |
| III-D38MA | 12 | 30.3 | 18.8 | 8.4 | 5.8 | 37.8 |
| III-D02MA | 15 | 27.5 | 17.3 | 9.1 | 8.8 | 37.0 |
| III-D08MA | 15 | 39.5 | 24.9 | 5.9 | 5.9 | 36.9 |
| III-302MA | 21 | 32.9 | 23.9 | 6.4 | 6.1 | 27.3 |
| III-303MA | 21 | 37.6 | 23.1 | 6.2 | 5.7 | 38.6 |

Age, age at examination; LVIDd, LV internal dimension diastolic; LVIDs, LV internal dimension systolic; IVS, intraventricular septum thickness; PW, posterior wall thickness; FS, fractional shortening

15 months and III-303MA at 21 months of age (data not shown). We found that the right ventricular walls were kept intact in all CXMD_J dogs examined.

Discussion

In electrocardiographic findings, an increased HR and a shortened PQ interval have been reported in both DMD patients [13] and GRMD [22]. These findings were also observed in CXMD_J dogs. Increased sympathetic activity and decreased parasympathetic activity have been observed in DMD patients and are associated with disease progression [30]; therefore, autonomic dysfunction in dystrophin deficiency might affect these parameters. It has been reported that HR is negatively correlated with PQ interval in normal Beagle dogs and it may be ascribed to a parasympathetic input at the level of the AV node [31]. The negative correlation between HR and PQ intervals was also found in affected dogs, indicating the parasympathetic input was maintained well even in affected dogs at AV node level. The QRS duration was within normal limits in the CXMD_J dogs, which is compatible with most cases of DMD [13]. Another peculiar electrocardiographic finding in DMD is the deep and narrow Q-waves in I, aVL and V6 or in II, III and aVF [10,13,16,32]. CXMD_J dogs also showed prominent Q-waves and increases in the Q/R ratio in leads II, III, and aVF, findings that are consistent with those in GRMD [23]. In all CXMD_J dogs examined, the distinct deep Q-waves were recognized by 6–7 months of age, which is earlier than the other abnormal electrocardiographic parameters, and the Q/R ratio in affected dogs remained high from 6 to 21 months of age. Actually, the prominent Q-wave and increase in Q/R ratio were also detected in some of the CXMD_J dogs at around 2 months of age (Fig. 1C), but it is difficult to evaluate the degree of the Q/R ratio increase before 3 months of age because the

QRS vector is almost exclusively directed to the right and varies significantly in the weeks after birth [33]. A previous report described GRMD dogs ranging from 6 months to > 2 years as having deep Q-waves and increased Q/R ratios in leads II, III, and aVF [23]. The Q-waves, however, might have been seen earlier and regarded as normal variants or not have been considered important for the reasons mentioned above.

Hyperechoic lesions indicating myocardial fibrosis in the posterobasal left ventricular wall have been detected by echocardiography in GRMD dogs as well as DMD patients [22,23]. Moise *et al.* reported that hyperechoic lesions were first detected in eight of eleven GRMD dogs (73%) by 6–7 months of age and that they correlated with histologically recognizable areas of mineralization and corresponded to the progression of fibrosis [23]. In our study, one of eight of CXMD_J dogs showed a hyperechoic lesion in the left ventricular posterior wall, but the rest had not by the age of 6–7 months (Table 3, Fig. 4). The hyperechoic lesion in the left ventricular posterior walls was detected in both III-302MA and III-303MA, but not early as 12 months of age (Table 3). The results of echocardiography indicated that the cardiac involvement in CXMD_J is milder than that in GRMD. Echocardiography did not reveal particular left ventricular dysfunction in any CXMD_J dog by 21 months of age, but a mild hypokinesis of the left ventricular wall was observed in III-302MA at 21 months of age (Fig. 3B). The dysfunction found in the dog, however, was mild and the dog had no cardiac symptoms. Moise *et al.* reported that three of the six GRMD dogs > 2 years of age showed a decrease in fractional shortening, but did not mention at what age the abnormal cardiac findings appeared.

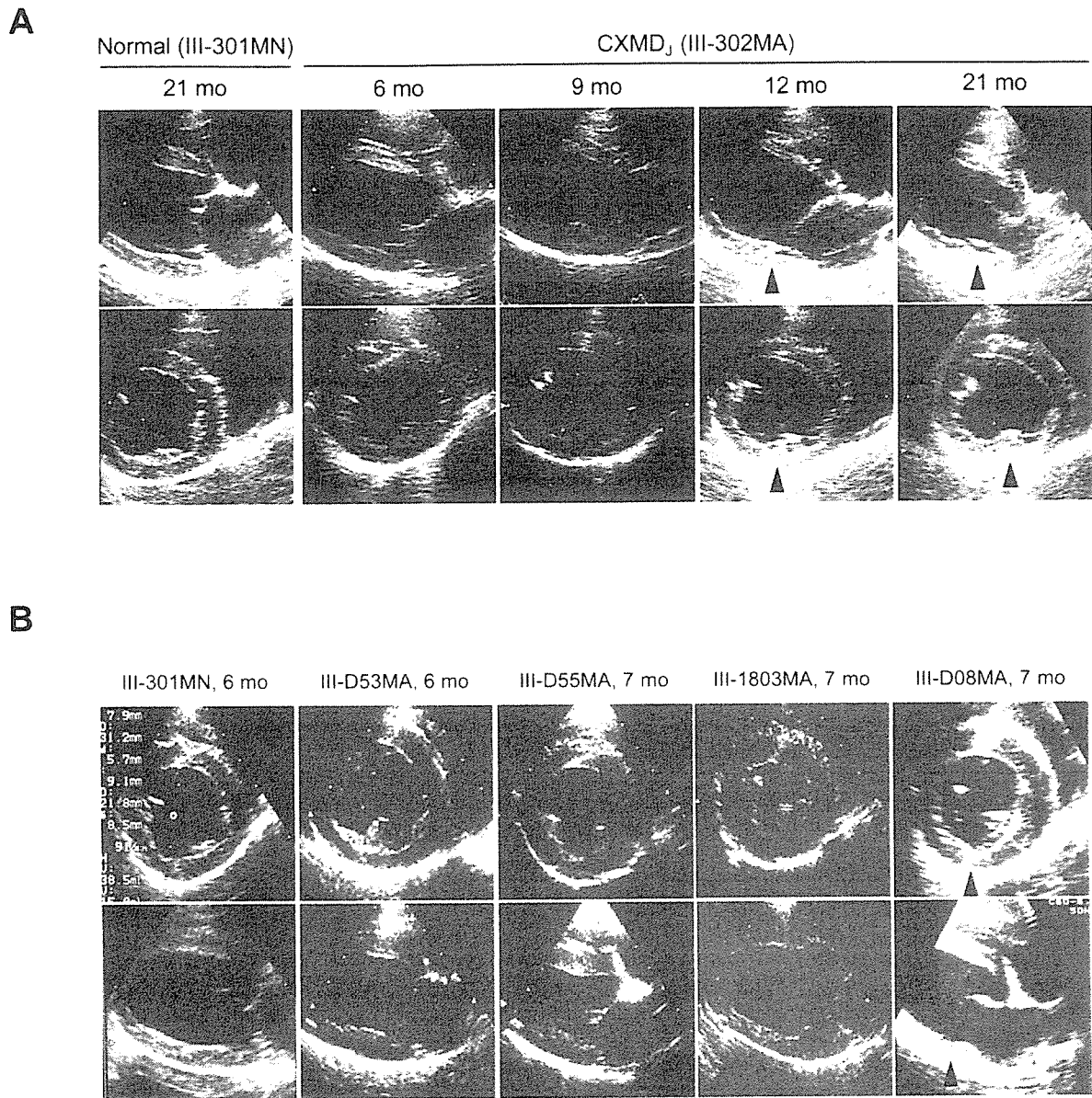


Figure 4
Echogenicity in CXMD. **A:** Sequential studies in echogenicity with advancing age by two-dimensional echocardiography in a normal dog III-301MN, and a CXMD_J dog III-302MA, at 6–21 months of age. Hyperechoic lesions (arrowheads) of the left ventricular posterior wall were detected in the CXMD_J dog at 12 months of age and older. **B:** Two-dimensional echocardiograms of a normal dog III-301MN at 6 months of age, and four CXMD_J dogs III-D53MA, III-D55MA, III-1803MA, and III-D08MA at 6 to 7 months of age. The hyperechoic lesion (arrowhead) was detected only in the left ventricular posterior wall of III-D08MA.

Previous studies of morphology in GRMD showed that myocardial involvement is initially found in the left pos-

terobasal ventricular wall, similar to that of patients with DMD [21-23]. Valentine *et al.* reported that GRMD dogs

Table 3: Echogenicity of left ventricular posterior wall in normal and CXMD_J male dogs

| | Months of age (mo) | | | | | | | | | | | | | | | | | | | | |
|------------------------------|--------------------|-----|-----|-----|------|------|---|-----|-----|----|------|-----|------|------|----|----|-----|----|----|------|--|
| | 2 | 3 | 4 | 5 | 6 | 7 | 8 | 9 | 10 | 11 | 12 | 13 | 14 | 15 | 16 | 17 | 18 | 19 | 20 | 21 | |
| Normal dogs | | | | | | | | | | | | | | | | | | | | | |
| III-D56MN | | | | | (-)* | | | | | | | | | | | | | | | | |
| III-1804MN | | | | | (-) | (-)* | | | | | | | | | | | | | | | |
| III-D03MN | (-) | | | (-) | | (-) | | | (-) | | | (-) | (-)* | | | | | | | | |
| III-301 MN | (-) | (-) | (-) | | (-) | | | (-) | | | (-) | | | (-) | | | (-) | | | (-)* | |
| CXMD_J dogs | | | | | | | | | | | | | | | | | | | | | |
| III-D53MA | | | | | (-)* | | | | | | | | | | | | | | | | |
| III-D55MA | | | | | | (-) | | * | | | | | | | | | | | | | |
| III-1803MA | | | | | (-) | (-)* | | | | | | | | | | | | | | | |
| III-D38MA | | | | | | | | | | | (-)* | | | | | | | | | | |
| III-D02MA | (-) | | | (-) | | (-) | | | | | (-) | (-) | | (-)* | | | | | | | |
| III-D08MA | (-) | | | (+) | | (+) | | | | | (+) | (+) | | (+)* | | | | | | | |
| III-302MA | (-) | (-) | (-) | | (-) | | | (-) | | | (+) | | | (+) | | | (+) | | | (+)* | |
| III-303MA | (-) | (-) | (-) | | (-) | | | (-) | | | (+) | | | (+) | | | (+) | | | (+)* | |

Hyperechoic lesion +, positive; -, negative; Asterisk in each CXMD_J dog shows age at euthanasia.

at 6.5 months of age had acute severe lesions with focal myocardial mineralization associated macrophages and giant cells in the left ventricular papillary muscle and left ventricular wall [22]. Moreover, GRMD dogs at 12 months of age or older demonstrated prominent myocardial fibrosis in more widespread lesions [22]. The myocardial fibrosis of the left ventricular wall in the older stage of CXMD_J dogs was consistent with that in DMD patients and GRMD dogs. The change was detected at 15 months of age or older in the CXMD_J (III-D08MA, III-302MA, and III-303MA), although III-D08MA showed a hyperechoic lesion at 5 months of age or older (Table 3). The cardiac involvement in CXMD_J, therefore, was milder and slowly progressed than that in GRMD, although a longer period evaluation of large numbers of CXMD_J will be needed to conclude the mild cardiac phenotypes of CXMD_J.

Why is the cardiac involvement in CXMD_J milder than that in GRMD? Valentine *et al.* reported that skeletal muscle involvement in small dystrophic dogs was milder than that in large ones [19]. Several reports on dystrophic features have hypothesized that the clinical severity may be associated with growth rate [34] or muscle fiber diameter [35]. Living in a cage rather than running free could also affect the cardiac phenotypes of CXMD_J because physical exercise promotes cardiac involvement in dystrophin-deficient *mdx* mice [36]. The difference in the genetic background between GRMD, golden retriever and CXMD_J, Beagle might also affect the disease progression.

The prominent deep Q-waves seen in both DMD and GRMD have been attributed to a reduction in or a loss of electromotive force caused by scarring of the posterobasal

region of the left ventricle [8,9,17]. In our study, the deep Q-waves and increases in the Q/R ratio in CXMD_J preceded the lesions seen on echocardiogram and histopathology, as shown in Fig. 6. Considering this result, the origin of the distinctive Q-waves might not be associated with the myocardial lesion in the posterobasal left ventricular wall. It has recently been reported that expression of a transgene in *mdx* mice for neuronal nitric oxide synthase (nNOS), which occurs as a secondary loss in dystrophin deficiency, decreased cardiac inflammation and fibrosis resulting in amelioration of both cardiac function and electrocardiographic abnormalities, including deep Q-waves [37]. Perloff *et al.* suggested that the alteration of a particular ionic current by lack of specific membrane proteins associated with dystrophin might participate in electrocardiographic changes [17]. We will not therefore deny that minimal myocardial damage could be associated with the pathogenesis of deep Q-waves, but our results suggest that an investigation of the conduction and cardiovascular systems will also be needed to explore the pathophysiology of the deep Q-waves in dystrophin-deficient heart. In this regard, CXMD_J will be very useful to elucidate aspects of the dystrophin-deficient heart, but we may recognize that a longer period of time would be required to complete cardiac phenotypes in CXMD_J.

Conclusion

We demonstrated that the cardiac phenotypes of CXMD_J are comparable to but milder than those of GRMD. Furthermore, we found for the first time that the distinct deep Q-waves precede detection of the left ventricular posterobasal lesion by echocardiography or histopathology. CXMD_J may provide not only new insights into the mech-

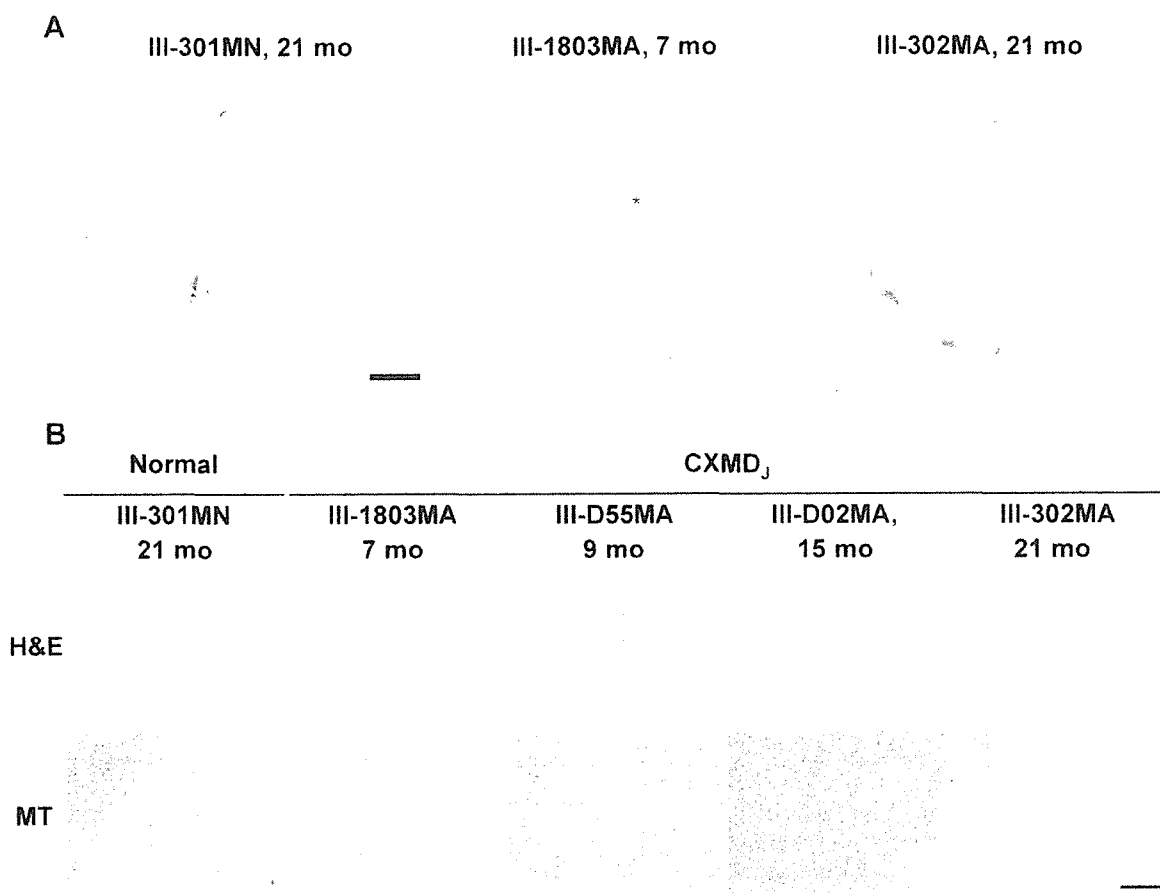


Figure 5
Macroscopic and histopathological findings in CXMD_j hearts **A.** Macroscopic examinations of the base of the formalin-fixed hearts of a normal littermate III-301MN at 21 months and CXMD_j dogs, III-1803MA at 7 months and III-302MA at 21 months of age. *Aortic valve. Bar shows 1 cm. **B.** Hematoxylin and eosin (H&E) and Masson's trichrome (MT) staining for histopathological evaluation of the left ventricular posterior wall in a normal littermate, III-301MN at 21 months and the CXMD_j dogs, III-1803MA at 7 months, III-D55MA at 9 months, III-D02MA at 15 months, and III-302MA at 21 months of age. Posterior walls of left ventricles of both III-D55MA and III-D02MA were macroscopically normal (data not shown). Bar shows 200 μm.

anisms causing the abnormal Q-waves but also more information on the pathogenesis in the dystrophin-deficient heart.

Competing interests

The author(s) declare that they have no competing interests.

Authors' contributions

NY and NU carried out the electrocardiographic, echocardiographic, and pathological examination and drafted the

manuscript. YF performed the electrocardiographic study. MY, KY and MRW participated in the necropsy and pathological examination. MN, YS, MT and AT participated in the maintenance of the dog colony and the design of the study. NM performed the pathological examination. YW participated in the design of the study. AN participated in the statistical analysis and drafted manuscript. ST participated in the design, planning and coordination of the study. All authors read and approved the final manuscript.

Acknowledgements

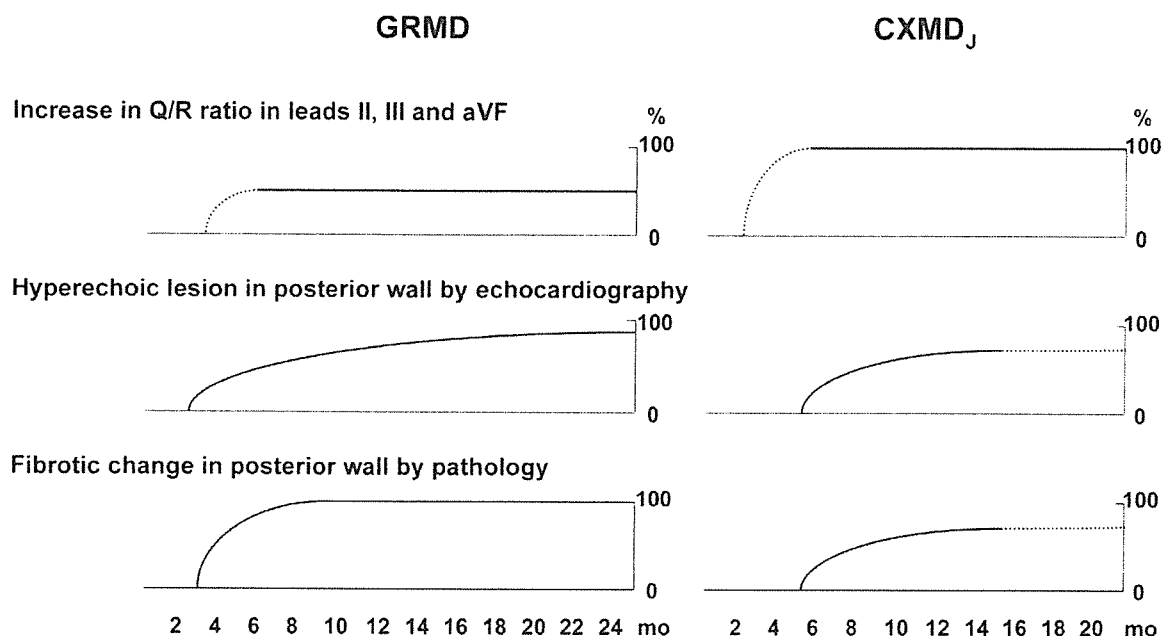


Figure 6

Comparison of cardiac involvement between GRMD and CXMD_j with advancing age. Subjects were compared as follows: increase in Q/R ratio in leads II, III, and aVF in ECG, hyperechoic lesion in posterior wall by echocardiography, and fibrotic change in left ventricular posterior wall by pathology. The data on GRMD was based on the previous literature [22–24]. It is difficult to evaluate Q/R ratio in early stage of GRMD and CXMD_j. It is also difficult to evaluate hyperechoic lesion in echocardiogram and fibrotic change in pathology at late stage of CXMD_j due to small numbers of examination (n < 3).

We thank Hideki Kita, Shin'ichi Ichikawa, Yumiko Yahata, and Kazue Kinoshita (JAC, Inc., Tokyo) for maintaining the dogs, Yoshikuni Tanioka (Central Institute for Experimental Animals, Kawasaki) for his support and valuable suggestions, and Ryoko Nakagawa (Department of Molecular Therapy, National Institute of Neuroscience, NCNP, Tokyo) for her technical assistance. This study was supported by Health Sciences Research Grants for Research on Psychiatric and Neurological Diseases and Mental Health (H12-kokoro-025, H15-kokoro-021, H18-kokoro-019), the Human Genome and Gene Therapy (H13-genome-001, H16-genome-003) from the Ministry of Health, Labor and Welfare of Japan, and Grants-in-Aid for Scientific Research from the Ministry of Education, Science, Sports and Culture of Japan (to S.T.).

References

- Koenig M, Hoffman EP, Bertelson CJ, Monaco AP, Feener C, Kunkel LM: **Complete cloning of the Duchenne muscular dystrophy (DMD) cDNA and preliminary genomic organization of the DMD gene in normal and affected individuals.** *Cell* 1987, **50**:509-517.
- Cullen MJ, Mastaglia FL: **Morphological changes in dystrophic muscle.** *Br Med Bull* 1980, **36**:145-152.
- Ervasti JM, Ohlendieck K, Kahl SD, Gaver MG, Campbell KP: **Deficiency of a glycoprotein component of the dystrophin complex in dystrophic muscle.** *Nature* 1990, **345**:315-319.
- Gilroy J, Cahalan JL, Berman R, Newman M: **Cardiac and pulmonary complications in Duchenne's progressive muscular dystrophy.** *Circulation* 1963, **27**:484-493.
- Moser H: **Duchenne muscular dystrophy: pathogenetic aspects and genetic prevention.** *Hum Genet* 1984, **66**:17-40.
- Mukoyama M, Kondo K, Hizawa K, Nishitani H: **Life spans of Duchenne muscular dystrophy patients in the hospital care program in Japan.** *J Neurol Sci* 1987, **81**:155-158.
- Eagle M, Baudouin SV, Chandler C, Giddings DR, Bullock R, Bushby K: **Survival in Duchenne muscular dystrophy: improvements in life expectancy since 1967 and the impact of home nocturnal ventilation.** *Neuromuscul Disord* 2002, **12**:926-929.
- Perloff JK, Roberts WC, de Leon AC Jr, O'Doherty D: **The distinct electrocardiogram of Duchenne's progressive muscular dystrophy. An electrocardiographic-pathologic correlative study.** *Am J Med* 1967, **42**:179-188.
- Sanyal SK, Johnson WW, Thapar MK, Pitner SE: **An ultrastructural basis for electrocardiographic alterations associated with Duchenne's progressive muscular dystrophy.** *Circulation* 1978, **57**:1122-1129.
- Perloff JK, de Leon AC Jr, O'Doherty D: **The cardiomyopathy of progressive muscular dystrophy.** *Circulation* 1966, **33**:625-648.
- Frankel KA, Rosser RJ: **The pathology of the heart in progressive muscular dystrophy: epimyocardial fibrosis.** *Hum Pathol* 1976, **7**:375-386.
- James TN: **Observation on the cardiovascular involvement, including the cardiac conduction system, in progressive muscular dystrophy.** *Am Heart J* 1962, **63**:48-56.

13. Finsterer J, Stöllberger C: **The heart in human dystrophinopathies.** *Cardiology* 2003, **99**:1-19.
14. Farah MG, Evans EB, Vignos PJ jr: **Echocardiographic evaluation of left ventricular function in Duchenne's muscular dystrophy.** *Am J Med* 1980, **69**:248-254.
15. D'Orsogna L, O'Shea JP, Miller G: **Cardiomyopathy of Duchenne muscular dystrophy.** *Pediatr Cardiol* 1988, **9**:205-213.
16. Perloff JK: **Cardiac rhythm and conduction in Duchenne's muscular dystrophy: a prospective study of 20 patients.** *J Am Coll Cardiol* 1984, **3**:1263-1268.
17. Perloff JK, Moise NS, Stevenson WG, Gilmour RF: **Cardiac electrophysiology in Duchenne muscular dystrophy: From basic science to clinical expression.** *J Cardiovasc Electrophysiol* 1992, **3**:394-409.
18. Goodwin FC, Muntoni F: **Cardiac involvement in muscular dystrophies: molecular mechanisms.** *Muscle Nerve* 2005, **32**:577-588.
19. Cooper BJ, Winand NJ, Stedman H, Valentine BA, Hoffman EP, Kunkel LM, Scott MO, Fischbeck KH, Kornegay JN, Avery RJ, Williams JR, Schmickel RD, Sylvester JE: **The homologue of the Duchenne locus is defective in X-linked muscular dystrophy of dogs.** *Nature* 1988, **334**:154-156.
20. Valentine BA, Cooper BJ, de Lahunta A, O'Quinn R, Blue JT: **Canine X-linked muscular dystrophy. An animal model of Duchenne muscular dystrophy: clinical studies.** *J Neurol Sci* 1988, **88**:69-81.
21. Valentine BA, Winand NJ, Pradhan D, Moise NS, de Lahunta A, Kornegay JN, Cooper BJ: **Canine X-linked muscular dystrophy as an animal model of Duchenne muscular dystrophy: a review.** *Am J Med Genet* 1992, **42**:352-356.
22. Valentine BA, Cummings JF, Cooper BJ: **Development of Duchenne-type cardiomyopathy. Morphologic studies in a canine model.** *Am J Pathol* 1989, **135**:671-678.
23. Moise NS, Valentine BA, Brown CA, Erb HN, Beck KA, Cooper BJ, Gilmour RF: **Duchenne's cardiomyopathy in a canine model: electrocardiographic and echocardiographic studies.** *J Am Coll Cardiol* 1991, **17**:812-820.
24. Shimatsu Y, Katagiri K, Furuta T, Nakura M, Tanioka Y, Yuasa K, Tomohiro M, Kornegay JN, Nonaka I, Takeda S: **Canine X-linked muscular dystrophy in Japan (CXMD).** *Exp Anim* 2003, **52**:93-97.
25. Shimatsu Y, Yoshimura M, Yuasa K, Urasawa N, Tomohiro M, Nakura M, Tanigawa M, Nakamura A, Takeda S: **Major clinical and histopathological characteristics of canine X-linked muscular dystrophy in Japan, CXMD.** *Acta Myol* 2005, **24**:145-154.
26. Honeyman K, Carville KS, Howell JM, Fletcher S, Wilton SD: **Development of a snapback method of single-strand conformation polymorphism analysis for genotyping Golden Retrievers for the X-linked muscular dystrophy allele.** *Am J Vet Res* 1999, **60**:734-737.
27. Tilley LP: **Basic canine and feline electrocardiography.** *Can Vet J* 1981, **22**:23-25.
28. Crippa L, Ferro E, Melloni E, Brambilla P, Cavalletti E: **Echocardiographic parameters and indices in the normal Beagle dog.** *Lab Anim* 1992, **26**:190-195.
29. Cornell CC, Kittleson MD, Della Torre P, Häggström J, Lombard CW, Pedersen HD, Vollmar A, Wey A: **Allometric scaling of M-mode cardiac measurements in normal adult dogs.** *J Vet Intern Med* 2004, **18**:311-321.
30. Yotsukura M, Fujii K, Katayama A, Tomono Y, Ando H, Sakata K, Ishihara T, Ishikawa K: **Nine-year follow-up study of heart rate variability in patients with Duchenne-type progressive muscular dystrophy.** *Am Heart J* 1998, **136**:289-296.
31. Hanton G, Rabemampianina Y: **The electrocardiogram of the beagle dog: reference values and effect of sex, genetic strain, body position and heart rate.** *Lab Anim* 2006, **40**:123-136.
32. Sanyal SK, Johnson WW: **Cardiac conduction abnormalities in children with Duchenne's progressive muscular dystrophy: electrocardiographic features and morphologic correlates.** *Circulation* 1982, **66**:853-863.
33. Trautvetter E, Detweiler DK, Patterson DF: **Evolution of the electrocardiogram in young dogs during the first 12 weeks of life.** *J Electrocardiol* 1981, **14**:267-273.
34. Zatz M, Betti RT: **Benign Duchenne muscular dystrophy in a patient with growth hormone deficiency.** *Am J Med Genet* 1986, **24**:567-572.
35. Braund KG, McGuire JA, Lincoln CE: **Observations on normal skeletal muscle of mature dogs: a cytochemical, histochemical, and morphometric study.** *Vet Pathol* 1982, **19**:577-595.
36. Nakamura A, Yoshida K, Takeda S, Dohi N, Ikeda S: **Progression of dystrophic features and activation of mitogen-activated protein kinases and calcineurin by physical exercise, in hearts of mdx mice.** *FEBS Lett* 2002, **520**:18-24.
37. Wehling-Henricks M, Jordan MC, Roos KP, Deng B, Tidball JG: **Cardiomyopathy in dystrophin-deficient hearts is prevented by expression of a neuronal nitric oxide synthase transgene in the myocardium.** *Hum Mol Genet* 2005, **14**:1921-1933.

Pre-publication history

The pre-publication history for this paper can be accessed here:

<http://www.biomedcentral.com/1471-2261/6/47/prepub>

Publish with **Bio Med Central** and every scientist can read your work free of charge

"BioMed Central will be the most significant development for disseminating the results of biomedical research in our lifetime."

Sir Paul Nurse, Cancer Research UK

Your research papers will be:

- available free of charge to the entire biomedical community
- peer reviewed and published immediately upon acceptance
- cited in PubMed and archived on PubMed Central
- yours — you keep the copyright

Submit your manuscript here:

http://www.biomedcentral.com/info/publishing_adv.asp



BioMedcentral

Functional heterogeneity of side population cells in skeletal muscle

Akiyoshi Uezumi, Koichi Ojima, So-ichiro Fukada, Madoka Ikemoto, Satoru Masuda, Yuko Miyagoe-Suzuki, Shin'ichi Takeda *

Department of Molecular Therapy, National Institute of Neuroscience, National Center of Neurology and Psychiatry, 4-1-1 Ogawa-higashi, Kodaira, Tokyo 187-8502, Japan

Received 18 December 2005
Available online 23 January 2006

Abstract

Skeletal muscle regeneration has been exclusively attributed to myogenic precursors, satellite cells. A stem cell-rich fraction referred to as side population (SP) cells also resides in skeletal muscle, but its roles in muscle regeneration remain unclear. We found that muscle SP cells could be subdivided into three sub-fractions using CD31 and CD45 markers. The majority of SP cells in normal non-regenerating muscle expressed CD31 and had endothelial characteristics. However, CD31⁻CD45⁻ SP cells, which are a minor subpopulation in normal muscle, actively proliferated upon muscle injury and expressed not only several regulatory genes for muscle regeneration but also some mesenchymal lineage markers. CD31⁻CD45⁻ SP cells showed the greatest myogenic potential among three SP sub-fractions, but indeed revealed mesenchymal potentials in vitro. These SP cells preferentially differentiated into myofibers after intramuscular transplantation in vivo. Our results revealed the heterogeneity of muscle SP cells and suggest that CD31⁻CD45⁻ SP cells participate in muscle regeneration.

© 2006 Elsevier Inc. All rights reserved.

Keywords: Side population cells; Muscle regeneration; Mesenchymal differentiation; Transplantation

Adult skeletal muscles have a remarkable ability to regenerate following muscle damage. This regeneration has been attributed to satellite cells that reside between the sarcolemma and the basal lamina. Satellite cells are quiescent mononucleated cells in normal conditions, however, in response to muscle damage, they become activated, proliferate, and then exit the cell cycle either to renew the quiescent satellite cell pool or to differentiate into mature myofibers. Thus, they have been considered to be the myogenic precursor cells that give rise to myoblasts and the sole source of adult myogenic cells [1].

In 1998, Ferrari et al. [2] have demonstrated for the first time that bone marrow (BM)-derived cells contribute to the skeletal muscle after BM transplantation. Side population (SP) cells were first identified in bone marrow based on the ability to exclude Hoechst 33342 dye as an enriched

fraction of hematopoietic stem cells (HSCs) [3], later, it has been reported that they also participate in muscle regeneration [4]. Studies using whole BM cells showed that BM-derived mononucleated cells display several characteristics of satellite cells, suggesting that donor-derived BM cells contribute to muscle fibers in a stepwise biological progression [5,6]. However, using single HSC transplantation experiment, Camargo et al. [7] suggested that cells committed to the myeloid lineage contribute to muscle through fusion event. Therefore, multiple mechanisms underlay contribution of BM-derived cells to skeletal muscle regeneration.

SP cells have been also identified in skeletal muscle [4]. Muscle SP cells cannot only reconstitute the hematopoietic system of lethally irradiated mice [4,8], but also differentiate into skeletal muscle cells [4,9]. Furthermore, they have been reported to participate in vascular regeneration [10]. Several lines of evidence suggest that muscle SP cells are a cell population distinct from satellite cells [9,11–13]. While muscle SP cells possess these attractive

* Corresponding author. Fax: +81 42 346 1750.
E-mail address: takeda@ncnp.go.jp (S. Takeda).

features, they have been reported to be heterogeneous population. In fact, muscle SP cells contain both CD45⁺ and CD45⁻ cells, and hematopoietic potential has been exclusively found in CD45⁺ fraction [8,9]. As regards the myogenic potential, both CD45⁺ and CD45⁻ fractions have been shown to differentiate into skeletal muscle cells [9,14], but there is no comparative study dealing with subpopulation of muscle SP cells during muscle regeneration.

In the present study, we have further divided muscle SP cells into three sub-fractions using CD31 and CD45, examined the properties of each sub-fraction, and identified a novel subpopulation (CD31⁻CD45⁻ SP cells) that showed the greatest myogenic potential both in vitro and in vivo. These results provide a new insight for stem cell-based therapy of muscular dystrophy.

Materials and methods

Animals. All procedures using experimental animals were approved by the Experimental Animal Care and Use Committee at the National Institute of Neuroscience. Eight- to ten-week-old C57BL/6 mice were purchased from Nihon CLEA (Japan). GFP Tg mice were provided by Dr. M. Okabe (Osaka University) and used in cell transplantation experiments. NOD/scid mice provided by the Institute for Experimental Animals, Japan, were used as recipients.

To induce muscle regeneration, 100 μ l of CTX (10 μ M in saline, Wako Chemicals) was injected into the tibialis anterior (TA) muscle with a 29-gauge needle. In FACS analysis experiments, CTX was injected into TA (50 μ l), gastrocnemius (50 μ l), and quadriceps femoris muscles (25 μ l).

BM transplantation was performed as previously described [14]. Mice were subjected to analysis 12 weeks after transplantation.

Antibodies. Mouse Bcrp-1 cDNA was provided by Dr. A.H. Schinkel [15]. A DNA fragment corresponding to cytoplasmic domain of Bcrp1, amino acids 300–337, was fused to GST in a pGEX-4T-2 vector (Amersham Biosciences), and the fusion protein was used to immunize rabbits. The serum obtained was affinity-purified. Other antibodies used in these studies are listed in Table S1.

Cell preparation and FACS analysis. Muscle-derived mononucleated cells were prepared from C57BL/6 mice, GFP Tg mice, or GFP-BM transplanted mice as previously described [14]. Hoechst staining was performed as described by Goodell et al. (http://www.bcm.tmc.edu/genetherapy/goodell/new_site/protocols.html). Cells were re-suspended at 10⁶ cells per ml in DMEM (Invitrogen) containing 2% FBS (Trace Biosciences), 10 mM Hepes, and 5 μ g/ml Hoechst 33342 (Sigma), and incubated for 90 min at 37 °C in the presence or the absence of 50 μ M verapamil (Sigma). During incubation, cells were mixed 3–4 times. For analysis of Ac-LDL uptake, 10 μ g/ml DiI-labeled Ac-LDL (Biomedical Technologies) was added. After antibody staining, cells were re-suspended in PBS containing 2.5% FBS and 2 μ g/ml propidium iodide (PI) (BD PharMingen). Cell sorting was performed on a FACS VantageSE flow cytometer (BD Biosciences). Debris and dead cells were excluded by forward scatter, side scatter, and PI gating. Cell viability after staining and sorting was comparable to that previously reported [14].

RNA extraction and RT-PCR. Total RNA was extracted from 1 \times 10⁴ FACS sorted cells by using a RNeasy Micro Kit (Qiagen) and then reverse transcribed into cDNA by using TaqMan Reverse Transcription Reagents (Roche). The PCRs were performed with 1 μ l cDNA product under the following cycling conditions: 94 °C for 3 min followed by 40 cycles of amplification (94 °C for 15 s, 60 °C for 30 s, and 72 °C for 30 s) with a final incubation at 72 °C for 5 min. Specific primer sequences used for PCR are available on request.

Cell culture. SP cells were cultured alone with growth medium (GM); DMEM containing 20% FBS and 2.5 ng/ml bFGF (Invitrogen) in chamber slides (Nalge Nunc) coated with Matrigel (BD Biosciences) for 3–5 days. For osteogenic differentiation, the medium was changed to a differentiation medium (DM), 5% horse serum in DMEM supplemented with or without 500 ng/ml recombinant human BMP2 (R&D Systems), and cultured for 4–6 days. For adipogenic differentiation, cells were exposed to 3 cycles of 3 days of adipogenic induction medium (Cambrex Bioscience) followed by 1 day of adipogenic maintenance medium (Cambrex Bioscience) and then cells were maintained for five more days in the adipogenic maintenance medium. Alkaline phosphatase (AP) was stained using Sigma kit #85 according to the manufacturer's instructions. To stain lipids, cells were fixed in 10% formalin, rinsed in water and then 60% isopropanol, stained with Oil red O in 60% isopropanol, and rinsed in water. For myogenic differentiation, muSP-31, muSP-45, or muSP-DN purified from GFP Tg mice were co-cultured with myoblasts prepared from C57BL/6 mice as previously described [16,17] in GM. DM was supplied 3–5 days after starting co-culture.

Osteogenic activity and myotube-forming activity were determined by the following formulas: osteogenic activity = [the number of AP⁺ cells in seven randomly selected fields (corresponding to one-tenth of the whole area of the well)]/(the number of seeded cells) and myotube-forming activity = (the number of GFP⁺ myotubes in seven randomly selected fields)/(the number of seeded cells). In order to measure the extent of adipogenic differentiation, stained oil droplets were extracted for 5 min with 100 μ l of 4% Nonidet P-40 in isopropanol, and the absorbance of the dye-triglyceride complex was measured at 520 nm [18]; then, adipogenic activity was determined by the following formula: (the absorbance at 520 nm)/(the number of seeded cells).

Intramuscular transplantation experiments. muSP-DN or muSP-31 cells were purified from GFP Tg mice and were injected directly into the TA muscles of NOD/scid mice. One day before transplantation, host TA muscles were treated with CTX. The number of transplanted cells is indicated in Table 1. Three weeks after transplantation, TA muscles were excised and fixed in 4% PFA for 30 min, immersed sequentially in 10% sucrose/PBS and 20% sucrose/PBS, and frozen in isopentane cooled with liquid nitrogen.

Immunohistochemistry. FACS sorted cells were collected by Cytospin3 (ThermoShandon). Cells were fixed with 4% PFA for 5 min. Frozen muscle tissues were sectioned using a cryostat. Specimens were blocked with 5% goat serum (Cedarlane) in PBS for 15 min and incubated with primary antibodies at 4 °C overnight, followed by secondary staining. Stained cells were mounted in Vectashield with DAPI (Vector) and photographed using a fluorescence microscope IX70 (OLYMPUS) equipped with a QuantixTM air-cooled CCD camera (Photometrics) and IP Lab software (Scanalytics Inc.). Stained muscle sections were counterstained with TOTO-3 (1:5000; Molecular Probes), then mounted in Vectashield (Vector), and observed under the confocal laser scanning microscope system TCSSP (Leica).

Statistics. Values were expressed as means \pm SD or \pm SEM. Statistical significance was assessed by Student's *t* test. In comparison of more than two groups, one-way analysis of variance (ANOVA) followed by the Fisher's PLSD was used. A probability of less than 5% ($P < 0.05$) or 1% ($P < 0.01$) was considered statistically significant.

Table 1
Appearance of GFP⁺ myofibers after intramuscular transplantation

| Cell type | Experiment No. | Number of injected cells/TA muscle | Number of GFP ⁺ myofibers/TA muscle |
|---------------|----------------|------------------------------------|--|
| muSP-DN cells | Ex. 1 | 1.7 \times 10 ³ | 14 |
| | Ex. 2 | 2.5 \times 10 ³ | 9 |
| | Ex. 3 | 2.5 \times 10 ³ | 0 |
| muSP-31 cells | Ex. 1 | 1.6 \times 10 ⁴ | 3 |
| | Ex. 2 | 1.6 \times 10 ⁴ | 0 |
| | Ex. 3 | 1.6 \times 10 ⁴ | 0 |

Results

Most muscle SP cells are found in a subset of capillary or vein endothelial cells in non-regenerating skeletal muscle

We identified verapamil-sensitive SP cells in skeletal muscle after Hoechst staining (Fig. 1A) and analyzed the expression of several markers on them. The majority of muscle SP cells were CD31⁺, usually recognized as a marker of endothelial cells (Figs. 1B–E), and negative for a pan-hematopoietic marker, CD45 (Fig. 1B). More than half of muscle SP cells were CD34⁺, and Sca-1⁺ cells comprised 90% of muscle SP cells (Figs. 1C and D). Compared to FACS profiles of whole-muscle-derived cells, SP cells were enriched in Sca-1⁺ cells (Fig. S1). More than 85% of muscle SP cells were CD31⁺ and took up acetylated low-density lipoprotein (Ac-LDL), a functional marker for endothelial cells and macrophages (Fig. 1E). These results indicate that most muscle SP cells have endothelial characteristics. Only cells in the main population (MP) were found to be Pax7⁺, indicating that SP cells do not include muscle satellite cells (data not shown).

To examine the localization of muscle SP cells, we generated a rabbit polyclonal anti-mouse Bcrp1 antibody, because it has been reported that Bcrp1 is the major determinant of the SP phenotype [19]. Our antibody clearly recognized Bcrp1 expression in liver, small intestine, and kidney, as previously reported (Fig. S2) [20,21]. We confirmed that Bcrp1 antibody recognizes more than 80% of SP cells and less than 3% of MP cells collected by cytopsin (Figs. 1F and G). In skeletal muscle, Bcrp1⁺ cells were found outside the muscle basal lamina (Fig. 1H), which clearly distinguished Bcrp1⁺ cells from satellite cells. Next, Bcrp1 expression in the vascular system was investigated. CD31 staining identified all endothelia from larger vessels to capillaries in muscle sections. Intriguingly, Bcrp1 was expressed by CD31-expressing endothelial cells, and its expression was preferentially observed on a subpopulation of capillary endothelium (Figs. 1I–K) and venous endothelium surrounded by thin vessel walls, as revealed by α -smooth muscle actin (α SMA) expression (Figs. 1L–N). These results, together with the results of FACS analysis, strongly suggest that the majority of muscle SP cells are a subset of endothelial cells present in capillaries or veins in non-regenerating skeletal muscle.

Behavior of muscle SP cells during muscle regeneration

We next examined the kinetics of SP cells during muscle regeneration induced by injection of cardiotoxin (CTX). After CTX injection, the total number of mononuclear cells per muscle weight gradually increased, with a peak at day 3. The number of SP cells also increased and reached its peak at day 3 (Fig. 2A). Muscle SP cells could be divided into three subpopulations based on CD31 and CD45 expression: CD31⁺CD45⁻ SP cells (designated muSP-31 cells), CD31⁻CD45⁺ SP cells (muSP-45 cells), and

CD31⁻CD45⁻ SP cells (muSP-DN cells). muSP-31 cells and muSP-DN cells distributed throughout the SP tail, but muSP-45 cells were located close to the shoulder (data not shown). The majority of muscle SP cells in untreated muscle were muSP-31 cells (Fig. 1B). During regeneration, however, muSP-45 cells and muSP-DN cells increased in both their ratios and their numbers (Figs. 2B and C). Although CD45⁺ cells were abundant in whole muscle-derived cells during regeneration and most of them were F4/80 antigen-positive mature macrophages, SP cells did not contain any mature inflammatory cells, as previously reported (data not shown) [14].

To clarify the origin of each subpopulation of SP cells, BM transplantation experiments were performed. We confirmed that muSP-45 cells were mobilized from bone marrow as previously reported (Figs. 3A and B) [14]. In contrast, both CD45⁻ SP fractions are residents of skeletal muscle (Figs. 3A and B), consistent with the results reported by Rivier et al. [22].

Next, to determine whether each subpopulation of SP cells proliferates in damaged muscle, cells were stained with Ki67 antibody. Most muSP-45 cells (Figs. 3C and D) and muSP-31 cells (Figs. 3G and H) prepared from regenerating muscle were negative for Ki67, suggesting that the proliferation activities of these two fractions were low. On the other hand, about 60% of muSP-DN cells were positive for Ki67 (Figs. 3E and F), indicating that muSP-DN cells actively proliferated during muscle regeneration.

We next examined Bcrp1 expression on three sub-fractionated SP cells and found that only muSP-31 cells were Bcrp1-positive (Fig. 3K). These results suggest that some ABC transporters other than Bcrp1 are responsible for the phenotype of CD31⁻ SP cells.

Gene expression of muscle SP cells during muscle regeneration

Our analysis revealed that each subpopulation of SP cells showed distinct kinetics during muscle regeneration. To better understand the traits of muscle SP cells, we analyzed gene expression during muscle regeneration. Three subpopulations of SP cells (in following experiments, muSP-45 cells from untreated muscle were omitted because of their low yield) or MP cells were collected from each time point during muscle regeneration, and RT-PCR was performed. We chose several myogenic (*Pax3*, *Pax7*, and *myf5*), endothelial (*Tie2*, *Flk1*, and *vWF*), and mesodermal-mesenchymal-associated (α SMA, *PPAR γ* , *Runx2*, *PDGFR α* , and *PDGFR β*) genes to clarify lineage characteristics of the target cells. We also examined expression of genes of developmental regulators (*msx1*, *Frizzled4* (*Fzd4*), *Patched1* (*Ptc1*), and *BMPRI1A*), angiogenic factors (*angiopoietin-1* (*ang1*) and *VEGF*), and TGF- β superfamily antagonists (*folliculin* and *DAN*). muSP-DN cells from untreated muscles expressed only *PDGFR β* , *Ptc1*, *ang1*, *folliculin*, and *DAN* (Fig. 4, cont, lane 1). Neither myogenic nor other lineage-specific markers could be detected in

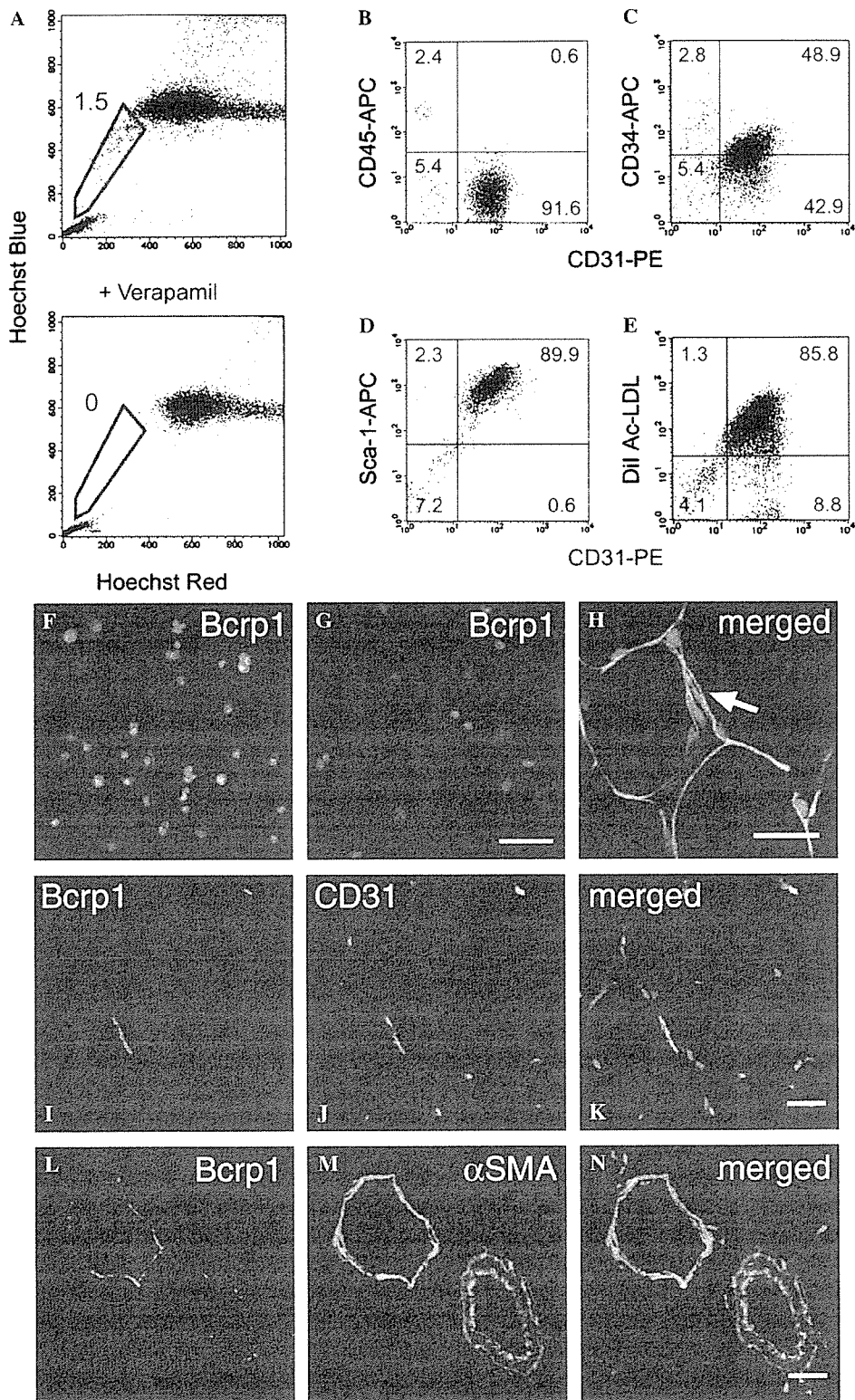


Fig. 1. Characterization of skeletal muscle SP cells. (A) Flow cytometric analysis of muscle-derived mononucleated cells after Hoechst 33342 staining with (lower panel) or without Verapamil (upper panel). The numbers indicate the percentage of SP cells (blue pentagons) in all mononucleated cells. (B–E) The expression of CD45 (B), CD34 (C), Sca-1 (D), and DiI-Ac-LDL uptake (E), and CD31 (B–E) on muscle SP cells. The percentage of cells in each quadrant is shown in the panel. (F,G) Immunofluorescent staining for Bcrp1 (green) and DAPI counterstaining (blue) of freshly sorted SP (F) and MP (G) cells. Immunofluorescent staining for Bcrp1 (green) and laminin $\alpha 2$ chain (red) (H), Bcrp1 (green) and CD31 (red) (I–K), and Bcrp1 (green) and α -smooth muscle actin (red) (L–N). TOTO-3 nuclear staining is shown in merged images (blue in H, K, and N). Bcrp1-positive cells are located outside the basal lamina (arrow), and they are partially overlapped with endothelial cells of capillary (I–K) and vein (L–N). Bars: 50 μ m in (F,G), 20 μ m in (H–N).

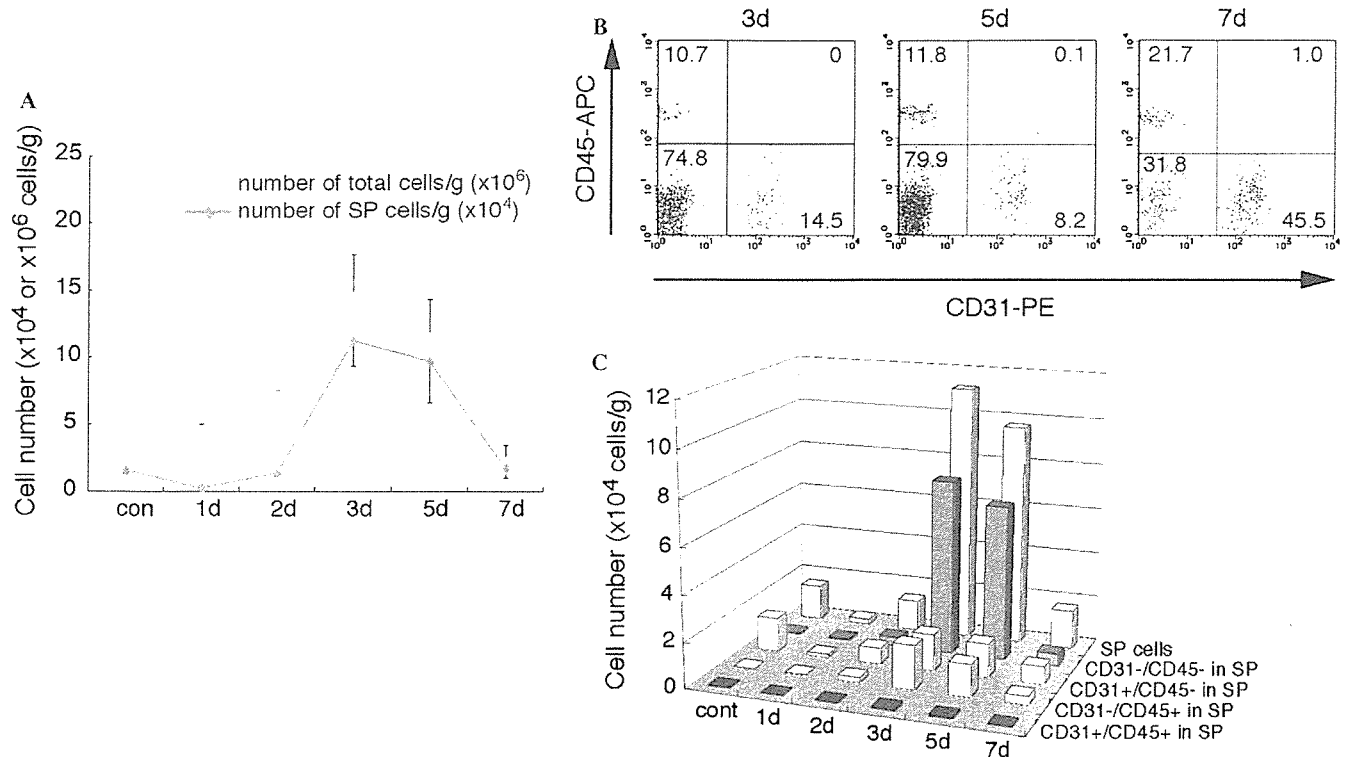


Fig. 2. Behavior of subpopulations of SP cells during muscle regeneration. (A) At 1 day (1d), 2 days (2d), 3 days (3d), 5 days (5d), and 7 days (7d) after CTX injection, the number of total cells (pink line) and SP cells (blue line) per gram of muscle weight was quantified. (B) At 3 days (3d), 5 days (5d), and 7 days (7d) after CTX injection, muscle SP cells prepared from regenerating muscle were analyzed for CD31 and CD45 expression. (C) Cell numbers in subpopulations of SP cells. muSP-45 cells (light blue bar) and muSP-DN cells (dark red bar) were significantly increased in number during muscle regeneration. Values (A,C) are the average of three independent experiments. Error bars represent SD.

this population indicating that muSP-DN cells do not contain cells committed to the lineages tested. At day 3 after CTX injection, muSP-DN cells began to express developmental regulator genes (Fig. 4, 3d, lane 1), and then at day 5, they also began to express several other lineage-specific genes (*Tie2*, α *SMA*, *PPAR γ* , and *Runx2*). Angiogenic factors and TGF- β superfamily antagonists were also strongly expressed at this time point (Fig. 4, 5d, lane 1). In contrast, muSP-31 cells continuously expressed all three endothelial genes analyzed throughout the regeneration process (Fig. 4, lane 2). Expression of mature endothelial marker, such as *vWF*, suggests that muSP-31 cells represent committed endothelial cells. muSP-45 cells expressed only low levels of α *SMA*, *PDGFR β* , and *follistatin* at day 5 after CTX injection (Fig. 4, lane 3). Myogenic markers, *Pax7* and *myf5*, were detected only in the MP fraction (Fig. 4, MP) indicating that myogenic cells are completely sorted into the MP fraction even during the process of muscle regeneration.

Differentiation potential of muscle SP cells for mesenchymal lineages

muSP-DN cells showed a unique gene expression pattern during muscle regeneration process: they began to express several mesenchymal genes at a late phase of muscle regeneration. Therefore, we examined the mesenchymal

potentials of muscle SP subpopulations. muSP-DN cells from untreated muscle readily gave rise to alkaline phosphatase (AP)-positive cells when cultured in the presence of bone morphogenetic protein 2 (BMP2) (Figs. 5A and C). With adipogenic induction, they also differentiated into adipocytes containing numerous lipid droplets in the cytoplasm (Figs. 5A and D). Reflecting the results of gene expression analysis, muSP-DN cells from regenerating muscle more efficiently differentiated into osteogenic cells and adipocytes than those from untreated muscle did (Figs. 5B–D). Unexpectedly, muSP-DN cells from regenerating muscle also differentiated into adipocytes without adipogenic induction (Figs. 5B and D), suggesting that they are susceptible to adipogenesis under our culture condition. In contrast, muSP-31 cells did not possess these differentiation potentials (Figs. 5A–D). Nor did muSP-45 cells, which were dramatically mobilized from BM into regenerating muscle (Figs. 5B–D). The attribute of differentiation potential is therefore a feature of muSP-DN.

Myogenic potential of muscle SP cells in vitro

We next evaluated the myogenic potential of muscle SP cells in vitro. When SP cells were cultured alone, they never differentiated into skeletal muscle cells (data not shown). Each subpopulation of SP cells was prepared from GFP Tg mice and co-cultured with wild type (WT) primary

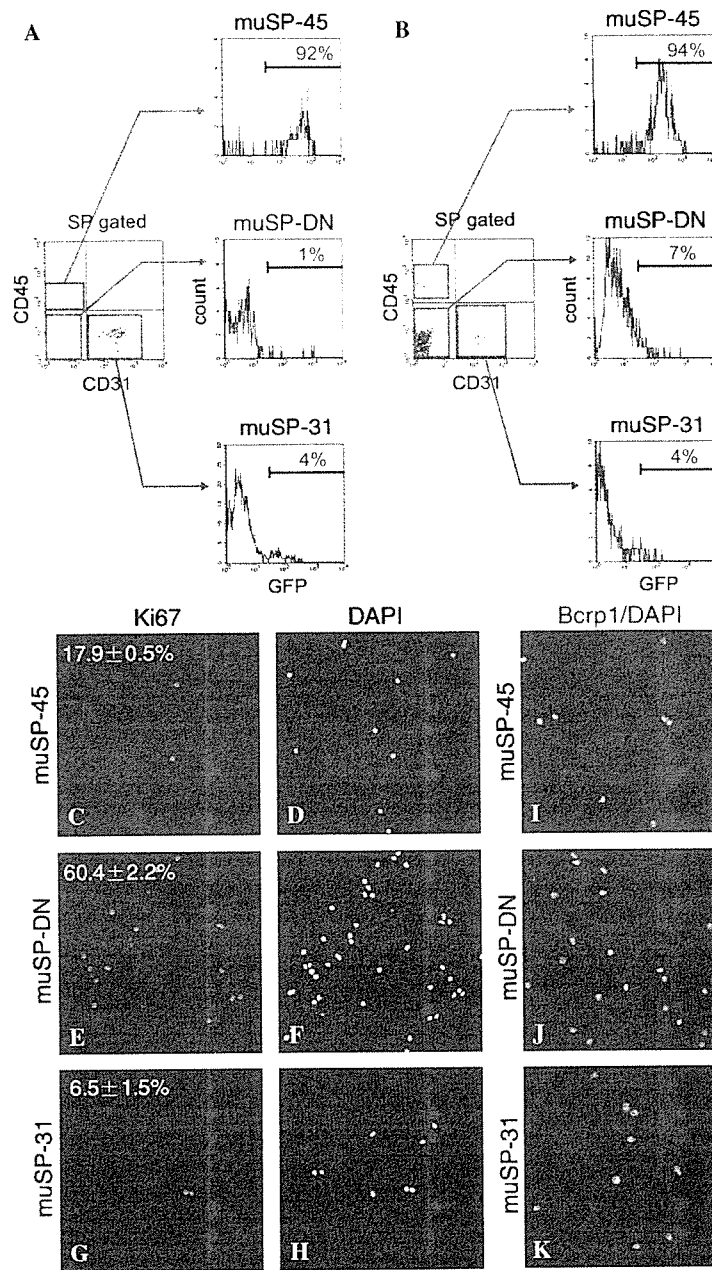


Fig. 3. Origin, proliferative activity, and Bcrp1 expression of subpopulations of muscle SP cells. (A,B) C57BL/6 mice were transplanted with whole BM from GFP Tg mice, and 3 months later, SP cells from untreated muscle (A) or regenerating muscle (3 days after CTX injection) (B) were further analyzed for CD31, CD45, and GFP expression. Note that CD45⁻ SP cells (middle and lower panels) are almost all negative for GFP, indicating that they do not originate from BM. In contrast, more than 90% of muSP-45 cells were GFP⁺ (upper panels). (C–H) Ki67 expression (green) and nuclei stained with DAPI (blue) on muSP-45 (C,D), muSP-DN (E,F), and muSP-31 (G,H) cells. The percentages of Ki67-positive cells were expressed as means \pm SD of three independent experiments. muSP-45 (I), muSP-DN (J), and muSP-31 (K) were sorted from regenerating muscle and stained for Bcrp1 (green) and nuclei (blue). Only muSP-31 cells were stained positive for Bcrp1 (K). Bar: 50 μ m.

myoblasts derived from satellite cells. muSP-DN cells from untreated muscle rapidly proliferated *in vitro* as observed in regenerating muscle (Fig. 2C). On the contrary, muSP-31 cells hardly expanded. After 2–3 weeks co-culture, both muSP-DN cells and muSP-31 cells differentiated not only into multinucleated myotubes co-expressing GFP and sarcomeric- α -actinin (Figs. 5E–G, only muSP-DN culture is shown) but also mononucleated myocytes (shown in insets). The frequency of mononucleated

myocytes was too low to quantify, but existence of these cells suggests that myogenic differentiation of SP cells could occur without fusion. Strikingly, the myotube-forming activity (the frequency of GFP⁺ myotubes, see Materials and methods for details) of muSP-DN cells was approximately 10-fold that of muSP-31 cells (Fig. 5H, lane for cont, 0.026 ± 0.007 vs 0.002 ± 0.001). In the experiments using SP cells from regenerating muscle at 3 days after CTX injection, muSP-DN cells showed the highest

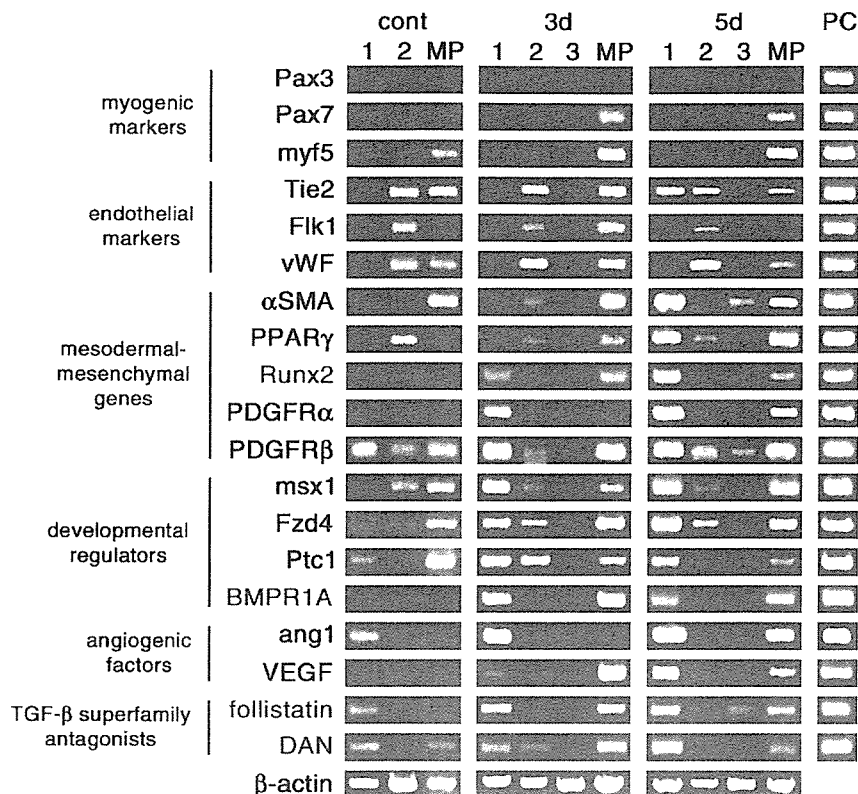


Fig. 4. Gene expression profiles of muscle SP cells during muscle regeneration. muSP-DN (lane 1), muSP-31 (lane 2), muSP-45 (lane 3), or MP cells were collected from untreated (cont) and regenerating muscle at 3 days (3d) or 5 days (5d) after CTX injection, and RT-PCR was performed against the indicated genes. Total embryo extract (E13) was used as a positive control (PC). β -actin was amplified to confirm that the quantities of mRNA were equal.

myotube-forming activity, although each SP subpopulation did form myotubes co-expressing GFP and sarcomeric- α -actinin (Fig. 5H, lane for CTX3d). This clearly demonstrates that muSP-DN cells have the highest myogenic potential among SP sub-fractions *in vitro*. For comparison, we quantified the myotube-forming activity of satellite cell-derived myoblasts. The value was 0.09 ± 0.01 , indicating that myogenic activity of myoblasts is much higher than that of muSP-DN cells.

Myogenic potential of muscle SP cells *in vivo*

To evaluate the myogenic potential of muscle SP cells *in vivo*, we performed transplantation experiments. muSP-DN or muSP-31 cells from untreated muscle of GFP Tg mice were directly transplanted into CTX-treated TA muscles of immunodeficient NOD/*scid* mice. Three weeks after transplantation, muSP-DN cells had generated myofibers more efficiently than muSP-31 cells (Figs. 6A and B, and Table 1), indicating that muSP-DN cells had relatively higher myogenic potential *in vivo* as well as *in vitro*. Contrary to our expectation, muSP-DN cells formed no GFP-positive adipocytes after transplantation.

Discussion

Muscle SP cells have been suggested to be multipotent and can contribute to skeletal muscle regeneration

[4,9,10,23]. However, most of these studies dealt with whole muscle SP cells as one functional unit. We subdivided, for the first time, muscle SP cells using CD31 and CD45 markers and revealed functional heterogeneity of muscle SP cells. CD31⁺CD45⁻ SP cells (muSP-31 cells) are a main subpopulation in non-regenerating muscle, but CD31⁻CD45⁻ SP cells (muSP-DN cells) which represent a minor subpopulation in non-regenerating muscle have the greatest differentiation potentials and become predominant subpopulation of SP cells upon muscle injury.

Differentiation potential of muscle SP cells

Phenotypic and immunohistochemical analysis suggested that muSP-31 cells are a subset of endothelial cells of capillaries and veins. They poorly proliferate after injury or in *in vitro* culture, and their differentiation potentials are limited both *in vitro* and *in vivo*.

CD45⁺ muscle SP cells (muSP-45 cells) were shown to have both hematopoietic and myogenic potentials, and hematopoietic potential of muscle-derived cells was exclusively found in this fraction [8,9]. We previously reported the contribution of muSP-45 cells to muscle regeneration [14]. In this study, we identified novel subpopulation that possesses much higher myogenic potential than muSP-45, muSP-DN.

muSP-DN cells showed the highest differentiation potential of all the mesenchymal lineages tested among

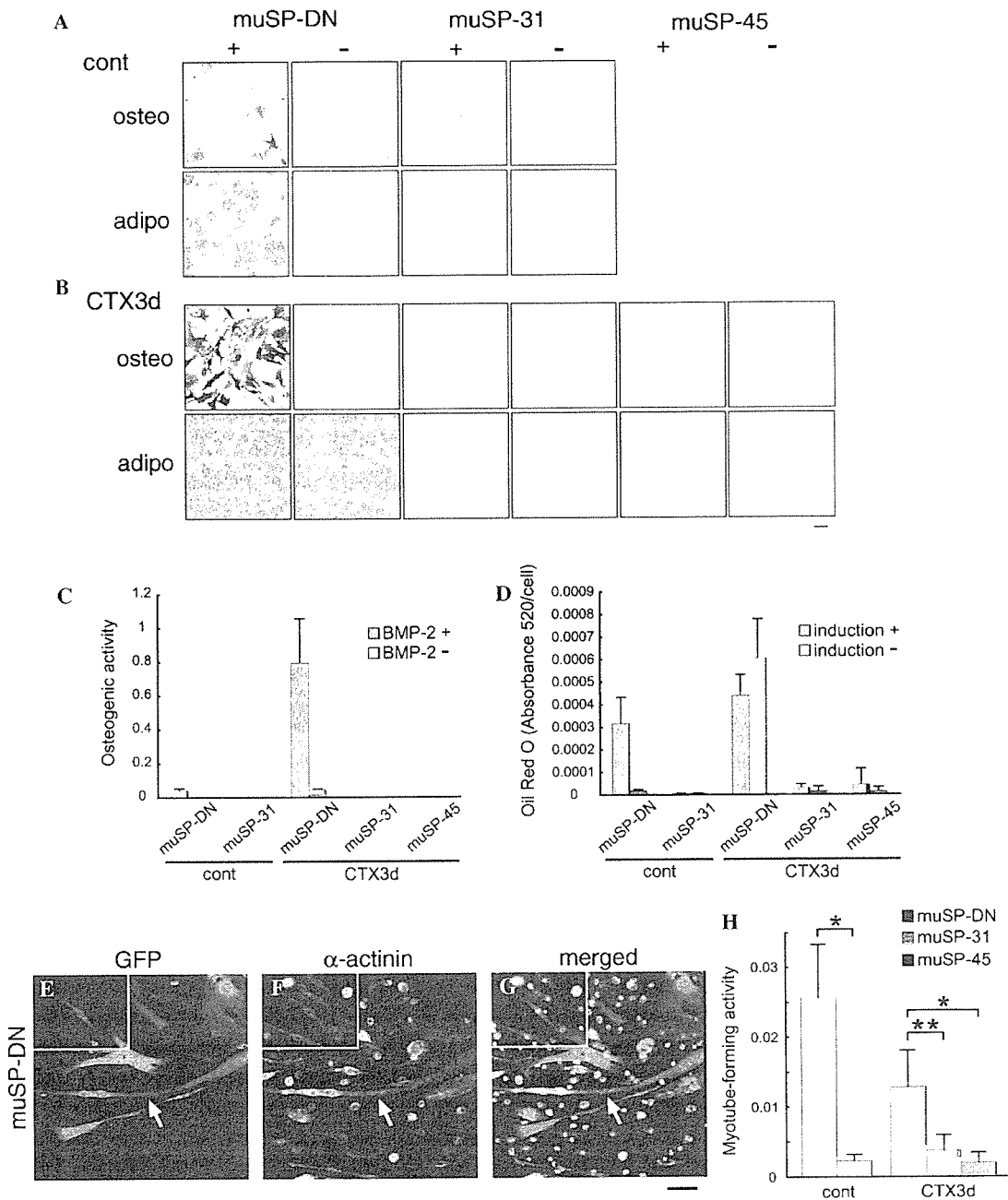


Fig. 5. muSP-DN cells differentiate into osteogenic cells, adipocytes, and skeletal muscle cells. (A,B) Three subpopulations of SP cells prepared from untreated (A) or regenerating (B) muscle were induced to differentiate into osteogenic or adipogenic cells. Uninduced cells (-) and induced cells (+) were then examined for alkaline phosphatase expression (osteo) or oil deposits (adipo). Bar: 50 μ m. (C,D) Osteogenic (C) and adipogenic (D) activities of subsets of SP cells prepared from control (cont) or regenerating muscle at 3 days after CTX injection (CTX3d) were quantified. Values are the average of three independent experiments. Error bars represent SD. (E-G) Co-culture of muscle SP cells with myoblasts. muSP-DN cells from GFP Tg mice were sorted and co-cultured with WT primary myoblasts in differentiation medium. Cells were stained with anti-GFP (green) and anti-sarcomeric α -actinin (red) antibodies. Nuclear staining with DAPI (blue) is shown in merged images (G). Insets show GFP⁺ mononucleated myocyte. Bar: 50 μ m. (H) Myotube-forming activities of muSP-DN cells (red bars), muSP-31 cells (blue bars), and muSP-45 cells (green bar) are shown. Each subpopulation was prepared from untreated (cont) or CTX-treated regenerating muscle (CTX3d). Values are the average of three independent experiments. Error bars represent SD. * $P < 0.01$, ** $P < 0.05$.

SP subpopulations. They were negative for lineage-specific markers under the non-regenerating condition, but after muscle injury or in in vitro expansion, they actively proliferated and were readily induced to express several mesenchymal genes. Their differentiation potential seems to be restricted to mesenchymal lineages because we did not

detect hematopoietic colonies derived from muSP-DN cells in vitro and muSP-DN cells failed to rescue the lethally irradiated mice (data not shown). These observations indicate that muSP-DN cells are enriched for primitive mesenchymal cells. This notion is further supported by gene expression pattern of muSP-DN cells. muSP-DN cells

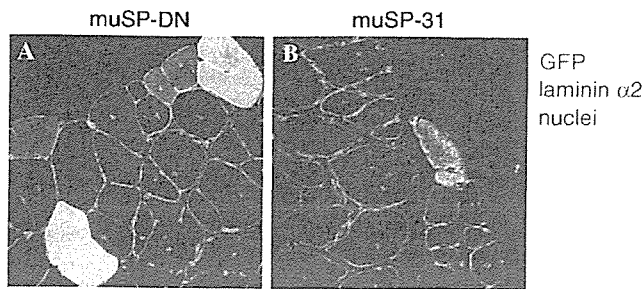


Fig. 6. muSP-DN cells participate in myofiber formation during muscle regeneration. (A,B) muSP-DN (A), muSP-31 (B) were transplanted into CTX-injected NOD/*scid* muscles. Each subpopulation was prepared from untreated muscle of GFP Tg mice. Muscle sections were stained with anti-GFP (green) and anti-laminin $\alpha 2$ (red) antibodies 3 weeks after transplantation. More GFP-positive myofibers were detected in muSP-DN-transplanted muscles (A) than in muscles transplanted with muSP-31 cells (B). Bar: 40 μ m.

specifically expressed *ang1* under the non-regenerating condition and during the early phase of regeneration (Fig. 4, lane 1, cont or 3d). Perivascular cells, such as pericytes, express *ang1* [24,25], and several groups suggest that multipotent mesenchymal stem cells may be derived from pericytes [26–28]. A recent report demonstrated that vascular mural precursor cells are negative for endothelial markers but positive for *Tie2* and smooth muscle cell markers [29]. Likewise, muSP-DN cells were negative for *Flk1* and *vWF* throughout the regeneration process (Fig. 4, lane 1), but began to express *Tie2* and α *SMA* during late phases of regeneration (Fig. 4, lane 1, 5d). Given the similarity between muSP-DN cells and those reported perivascular primitive cells, muSP-DN cells would represent perivascular primitive mesenchymal cells in skeletal muscle.

Roles of muscle SP cells in muscle regeneration

muSP-DN cells actively proliferated and significantly increased in number upon muscle injury. The precise fate of muSP-DN cells has remained to be determined, since the number of muSP-DN cells returned to normal level at late stage of muscle regeneration.

We noted that angiogenic factors and TGF- β superfamily antagonists were strongly expressed in muSP-DN cells during muscle regeneration. Previous reports showed that *Ptcl*⁺ interstitial mesenchymal cells in muscle produce angiogenic factors, including *ang1*, and promote muscle regeneration after ischemia [30,31]. Some members of the TGF- β superfamily, such as myostatin and TGF- β 1, are known to act as negative regulators of myogenesis [32,33]. Inversely, one of the TGF- β superfamily antagonists, follistatin, has been reported to promote myoblast recruitment and fusion [34]. Therefore, muSP-DN cells might promote muscle regeneration by producing regeneration-regulating factors.

muSP-DN cells preferentially differentiate into myogenic cells after intramuscular transplantation, implying that normal muscle environment facilitates myogenic differenti-

ation of muSP-DN cells. However, we revealed that muSP-DN cells have a high tendency to differentiate into osteogenic or adipogenic cells in vitro. Therefore, it is possible that muSP-DN cells differentiate into osteogenic or adipogenic cells in some pathological conditions such as Duchenne muscular dystrophy [35,36]. Recent finding that microvascular pericytes can differentiate into adipocytes [37] further supports the notion that muSP-DN cells might be implicated in pathological changes.

In conclusion, we identified novel subpopulation of muscle SP cells, CD31⁻CD45⁻ SP cells, which possesses capacity of mesenchymal differentiation in vitro and reveals myogenic differentiation potential in vivo. Our findings might provide new insights that may well be useful in understanding adult skeletal muscle regeneration and in designing therapeutic strategies of muscular dystrophy.

Acknowledgments

The authors are grateful to Ms. A. Fukase for technical assistance, and colleagues in Department of Molecular Therapy, especially Dr. M. Imamura, for useful discussion and suggestions on this work. This work is supported by Grants-in-Aid for Center of Excellence (COE), Research on Nervous and Mental Disorders (13B-1, 16B-2), and Health Science Research Grants for Research on the Human Genome and Gene Therapy (H13-genome-001, H16-genome-003), for Research on Brain Science (H12-Brain-025, H15-Brain-021) from the Ministry of Health, Labor and Welfare, Grants-in-Aids for Scientific Research (14657158, 15390281, and 16590333) from the Ministry of Education, Culture, Sports, Science and Technology, and a Research Grant from National Space Development Agency of Japan (NASDA) and the Japan Space Forum.

Appendix A. Supplementary data

Supplementary data associated with this article can be found, in the online version, at doi:10.1016/j.bbrc.2006.01.037.

References

- [1] R. Bischoff, Satellite and stem cells in muscle regeneration, in: A.G. Engel, C. Franzini-Armstrong (Eds.), *Myology*, McGraw-Hill, New York, 2004, pp. 66–86.
- [2] G. Ferrari, G. Cusella-De Angelis, M. Coletta, E. Paolucci, A. Stornaiuolo, G. Cossu, F. Mavilio, Muscle regeneration by bone marrow-derived myogenic progenitors, *Science* 279 (1998) 1528–1530.
- [3] M.A. Goodell, K. Brose, G. Paradis, A.S. Conner, R.C. Mulligan, Isolation and functional properties of murine hematopoietic stem cells that are replicating in vivo, *J. Exp. Med.* 183 (1996) 1797–1806.
- [4] E. Gussoni, Y. Soneoka, C.D. Strickland, E.A. Buzney, M.K. Khan, A.F. Flint, L.M. Kunkel, R.C. Mulligan, Dystrophin expression in the mdx mouse restored by stem cell transplantation. *Nature* 401 (1999) 390–394.
- [5] S. Fukada, Y. Miyagoe-Suzuki, H. Tsukihara, K. Yuasa, S. Higuchi, S. Ono, K. Tsujikawa, S. Takeda, H. Yamamoto, Muscle regener-

- ation by reconstitution with bone marrow or fetal liver cells from green fluorescent protein-gene transgenic mice, *J. Cell Sci.* 115 (2002) 1285–1293.
- [6] M.A. LaBarge, H.M. Blau, Biological progression from adult bone marrow to mononucleate muscle stem cell to multinucleate muscle fiber in response to injury, *Cell* 111 (2002) 589–601.
- [7] F.D. Camargo, R. Green, Y. Capetanaki, K.A. Jackson, M.A. Goodell, Single hematopoietic stem cells generate skeletal muscle through myeloid intermediates, *Nat. Med.* 9 (2003) 1520–1527.
- [8] S.L. McKinney-Freeman, S.M. Majka, K.A. Jackson, K. Norwood, K.K. Hirschi, M.A. Goodell, Altered phenotype and reduced function of muscle-derived hematopoietic stem cells, *Exp. Hematol.* 31 (2003) 806–814.
- [9] A. Asakura, P. Seale, A. Girgis-Gabardo, M.A. Rudnicki, Myogenic specification of side population cells in skeletal muscle, *J. Cell Biol.* 159 (2002) 123–134.
- [10] S.M. Majka, K.A. Jackson, K.A. Kienstra, M.W. Majesky, M.A. Goodell, K.K. Hirschi, Distinct progenitor populations in skeletal muscle are bone marrow derived and exhibit different cell fates during vascular regeneration, *J. Clin. Invest.* 111 (2003) 71–79.
- [11] E. Bachrach, S. Li, A.L. Perez, J. Schienda, K. Liadaki, J. Volinski, A. Flint, J. Chamberlain, L.M. Kunkel, Systemic delivery of human microdystrophin to regenerating mouse dystrophic muscle by muscle progenitor cells, *Proc. Natl. Acad. Sci. USA* 101 (2004) 3581–3586.
- [12] S. Fukada, S. Higuchi, M. Segawa, K. Koda, Y. Yamamoto, K. Tsujikawa, Y. Kohama, A. Uezumi, M. Imamura, Y. Miyagoe-Suzuki, S. Takeda, H. Yamamoto, Purification and cell-surface marker characterization of quiescent satellite cells from murine skeletal muscle by a novel monoclonal antibody, *Exp. Cell Res.* 296 (2004) 245–255.
- [13] P. Seale, L.A. Sabourin, A. Girgis-Gabardo, A. Mansouri, P. Gruss, M.A. Rudnicki, Pax7 is required for the specification of myogenic satellite cells, *Cell* 102 (2000) 777–786.
- [14] K. Ojima, A. Uezumi, H. Miyoshi, S. Masuda, Y. Morita, A. Fukase, A. Hattori, H. Nakauchi, Y. Miyagoe-Suzuki, S. Takeda, Mac-1^{low} early myeloid cells in the bone marrow-derived SP fraction migrate into injured skeletal muscle and participate in muscle regeneration, *Biochem. Biophys. Res. Commun.* 321 (2004) 1050–1061.
- [15] J.D. Allen, R.F. Brinkhuis, J. Wijnholds, A.H. Schinkel, The mouse Bcrp1/Mxr/Abcp gene: amplification and overexpression in cell lines selected for resistance to topotecan, mitoxantrone, or doxorubicin, *Cancer Res.* 59 (1999) 4237–4241.
- [16] T.A. Rando, H.M. Blau, Primary mouse myoblast purification, characterization, and transplantation for cell-mediated gene therapy, *J. Cell Biol.* 125 (1994) 1275–1287.
- [17] Z. Qu, L. Balkir, J.C. van Deutekom, P.D. Robbins, R. Pruchnic, J. Huard, Development of approaches to improve cell survival in myoblast transfer therapy, *J. Cell Biol.* 142 (1998) 1257–1267.
- [18] R. Kasturi, V.C. Joshi, Hormonal regulation of stearyl coenzyme A desaturase activity and lipogenesis during adipose conversion of 3T3-L1 cells, *J. Biol. Chem.* 257 (1982) 12224–12230.
- [19] S. Zhou, J.D. Schuetz, K.D. Bunting, A.M. Colapietro, J. Sampath, J.J. Morris, I. Lagutina, G.C. Grosveld, M. Osawa, H. Nakauchi, B.P. Sorrentino, The ABC transporter Bcrp1/ABCG2 is expressed in a wide variety of stem cells and is a molecular determinant of the side-population phenotype, *Nat. Med.* 7 (2001) 1028–1034.
- [20] M. Maliepaard, G.L. Scheffer, I.F. Faneyte, M.A. van Gastelen, A.C. Pijnenborg, A.H. Schinkel, M.J. van De Vijver, R.J. Scheper, J.H. Schellens, Subcellular localization and distribution of the breast cancer resistance protein transporter in normal human tissues, *Cancer Res.* 61 (2001) 3458–3464.
- [21] J.W. Jonker, M. Buitelaar, E. Wagenaar, M.A. Van Der Valk, G.L. Scheffer, R.J. Scheper, T. Plosch, F. Kuipers, R.P. Elferink, H. Rosing, J.H. Beijnen, A.H. Schinkel, The breast cancer resistance protein protects against a major chlorophyll-derived dietary phototoxin and protoporphyria, *Proc. Natl. Acad. Sci. USA* 99 (2002) 15649–15654.
- [22] F. Rivier, O. Alkan, A.F. Flint, K. Muskiewicz, P.D. Allen, P. Le Boulch, E. Gussoni, Role of bone marrow cell trafficking in replenishing skeletal muscle SP and MP cell populations, *J. Cell Sci.* 117 (2004) 1979–1988.
- [23] A.P. Meeson, T.J. Hawke, S. Graham, N. Jiang, J. Elterman, K. Hutcheson, J.M. Dimairo, T.D. Gallardo, D.J. Garry, Cellular and molecular regulation of skeletal muscle side population cells, *Stem Cells* 22 (2004) 1305–1320.
- [24] S. Davis, T.H. Aldrich, P.F. Jones, A. Acheson, D.L. Compton, V. Jain, T.E. Ryan, J. Bruno, C. Radziejewski, P.C. Maisonpierre, G.D. Yancopoulos, Isolation of angiopoietin-1, a ligand for the TIE2 receptor, by secretion-trap expression cloning, *Cell* 87 (1996) 1161–1169.
- [25] N. Takakura, T. Watanabe, S. Suenobu, Y. Yamada, T. Noda, Y. Ito, M. Satake, T. Suda, A role for hematopoietic stem cells in promoting angiogenesis, *Cell* 102 (2000) 199–209.
- [26] M.J. Doherty, B.A. Ashton, S. Walsh, J.N. Beresford, M.E. Grant, A.E. Canfield, Vascular pericytes express osteogenic potential in vitro and in vivo, *J. Bone Miner. Res.* 13 (1998) 828–838.
- [27] M.M. Levy, C.J. Joyner, A.S. Virdi, A. Reed, J.T. Triffitt, A.H. Simpson, J. Kenwright, H. Stein, M.J. Francis, Osteoprogenitor cells of mature human skeletal muscle tissue: an in vitro study, *Bone* 29 (2001) 317–322.
- [28] S. Shi, S. Gronthos, Perivascular niche of postnatal mesenchymal stem cells in human bone marrow and dental pulp, *J. Bone Miner. Res.* 18 (2003) 696–704.
- [29] M. Iurlaro, M. Scatena, W.H. Zhu, E. Fogel, S.L. Wieting, R.F. Nicosia, Rat aorta-derived mural precursor cells express the Tie2 receptor and respond directly to stimulation by angiopoietins, *J. Cell Sci.* 116 (2003) 3635–3643.
- [30] R. Pola, L.E. Ling, M. Silver, M.J. Corbley, M. Kearney, R. Blake Pepinsky, R. Shapiro, F.R. Taylor, D.P. Baker, T. Asahara, J.M. Isner, The morphogen Sonic hedgehog is an indirect angiogenic agent upregulating two families of angiogenic growth factors, *Nat. Med.* 7 (2001) 706–711.
- [31] R. Pola, L.E. Ling, T.R. Aprahamian, E. Barban, M. Bosch-Marce, C. Curry, M. Corbley, M. Kearney, J.M. Isner, D.W. Losordo, Postnatal recapitulation of embryonic hedgehog pathway in response to skeletal muscle ischemia, *Circulation* 108 (2003) 479–485.
- [32] Y. Li, W. Foster, B.M. Deasy, Y. Chan, V. Prisk, Y. Tang, J. Cummins, J. Huard, Transforming growth factor-beta1 induces the differentiation of myogenic cells into fibrotic cells in injured skeletal muscle: a key event in muscle fibrogenesis, *Am. J. Pathol.* 164 (2004) 1007–1019.
- [33] A.C. McPherron, A.M. Lawler, S.J. Lee, Regulation of skeletal muscle mass in mice by a new TGF-beta superfamily member, *Nature* 387 (1997) 83–90.
- [34] S. Iezzi, M. Di Padova, C. Serra, G. Caretti, C. Simone, E. Maklan, G. Minetti, P. Zhao, E.P. Hoffman, P.L. Puri, V. Sartorelli, Deacetylase inhibitors increase muscle cell size by promoting myoblast recruitment and fusion through induction of follistatin, *Dev. Cell* 6 (2004) 673–684.
- [35] A.G. Engel, E. Ozawa, *Dystrophinopathies*, in: A.G. Engel, C. Franzini-Armstrong (Eds.), *Myology*, McGraw-Hill, New York, 2004, pp. 961–1025.
- [36] B.Q. Banker, A.G. Engel, *Basic reactions of muscle*, in: A.G. Engel, C. Franzini-Armstrong (Eds.), *Myology*, McGraw-Hill, New York, 2004, pp. 691–747.
- [37] C. Farrington-Rock, N.J. Crofts, M.J. Doherty, B.A. Ashton, C. Griffin-Jones, A.E. Canfield, Chondrogenic and adipogenic potential of microvascular pericytes, *Circulation* 110 (2004) 2226–2232.



Hormonal stimulation increases the recruitment of bone marrow-derived myoepithelial cells and periductal fibroblasts into the mammary gland [☆]

Takafumi Sangai ^{a,b}, Genichiro Ishii ^a, Hiroshi Fujimoto ^{a,b}, Akashi Ikehara ^a,
Takashi Ito ^{a,c}, Takahiro Hasebe ^a, Junji Magae ^d, Takeshi Nagashima ^b,
Masaru Miyazaki ^b, Atsushi Ochiai ^{a,c,*}

^a Pathology Division, Innovative Medical Research Center, National Cancer Center, 6-5-1 Kashiwanoha, Kashiwa-City, Chiba 277-8577, Japan

^b Department of General Surgery, Graduate School of Medicine, Chiba University, Chiba, Japan

^c Laboratory of Cancer Biology, Department of Integrated Biosciences, Graduate School of Frontier Sciences, The University of Tokyo, Chiba, Japan

^d Department of Biotechnology, Institute of Research and Innovation, Chiba, Japan

Received 22 May 2006

Available online 13 June 2006

Abstract

Recent reports have revealed that bone marrow (BM)-derived cells can be constituents in a number of organs, especially in remodeling tissue. Using bone marrow transplantation (BMT) technique, we found that BM can serve as a source of both myoepithelial cells and periductal fibroblasts in the mammary gland. The numbers of BM-derived myoepithelial cell were 4.8-fold, and those of periductal fibroblast were 2.4-fold higher in the mice when BMT which was performed at the pubertal stage, as compared with BMT was performed at the postpubertal stage. Treatment with estrogen + progesterone pellet increased numbers of BM-derived myoepithelial cells and periductal fibroblasts, to levels 4.5- and 2.6-fold higher than in placebo mice, respectively. *In situ* hybridization revealed BM-derived periductal fibroblasts expressed insulin-like growth factor I mRNAs that are known to regulate mammary gland. These results suggest that drastic structural change that is induced by hormonal stimulation increased the recruitment of BM-derived myoepithelial cells and periductal fibroblasts to the mammary gland context.

© 2006 Elsevier Inc. All rights reserved.

Keywords: Mammary gland; Bone marrow-derived cell; Myoepithelial cell; Periductal fibroblast

Cross-talk between the mammary epithelium and stromal cells is crucial for proper postnatal development of mammary gland [1,2]. The major components of the mammary gland are the mammary duct and the surrounding stroma. The mammary duct consists of two main cell types, luminal epithelial cells and monolayer myoepithelial cells,

surrounding them. Myoepithelial cells are highly specialized cells and are ultrastructurally reminiscent of smooth muscle cells [3]. They express contractile and cytoskeletal proteins such as α -smooth muscle actin (α -SMA). Cap cells are considered to elongate laterally along the duct and differentiate into myoepithelial cells [4–6], and this process is indispensable for the ductal branching in mammary gland development. The compartment outside the ductal tree contains adipose cells, fibroblasts, and immune cells. Periductal fibroblasts are located adjacent to the mammary epithelium within periductal stroma tissue. Previous reports describing fibroblasts in mammary glands as expressing several functional molecules [7–11], and bone marrow (BM)-derived, circulating cells (macrophages and eosinophils) rescued postnatal mammary gland development of

[☆] This work was supported by Grant-in-Aid for Cancer Research from the Ministry of Health and Welfare of Japan (15-13)(16-16) and a Grant-in-Aid for the Third Term Comprehensive 10-year Strategy for Cancer Control from the Ministry of Health and Welfare of Japan. T.S., H.F., and A.I. are Awardees of Research Resident Fellowships from the Foundation for Promotion of Cancer Research in Japan.

* Corresponding author. Fax: +81 4 7134 6865.

E-mail address: aochiai@east.ncc.go.jp (A. Ochiai).

sublethal irradiated mice [12]. These observations indicate that not only originally located cells but also circulating cells play essential role in normal development of mammary gland. Many recent reports showed it to be possible for BM to contain mesenchymal progenitor cells for skeletal muscle [13–15], heart [16–18], liver [19–21], and vascular cells [22,23]. Investigators including us have also revealed that BM-derived cells can serve as progenitors for tissue fibroblasts that are recruited through the circulation to populate peripheral organs [24,25], injured tissues [26,27], and cancer-induced stroma [28,29]. And these cells are more frequently recruited to remodeling tissue. It is well known that mammary gland morphology is markedly altered during postnatal growth by stimuli of hormones in combination with growth factors. In the present study, we used BM transplantation (BMT) and whole mammary gland transplantation (WMT) technique, and explored the hypothesis that BM-derived cells contribute to ductal morphogenesis as the progenitor cells of the mammary gland components in postnatal mammary gland development and the maintenance.

Materials and methods

Animal models. Transgenic mouse lines with an enhanced green fluorescence protein cDNA under the control of a chicken β -actin promoter and cytomegalovirus enhancer (GFP Tg; GFP+/- mice, C57BL/6) [30]; were purchased from The Jackson Laboratory (Bar Harbor, ME). After prenatal development, all of the tissues except for erythrocytes and hair from these transgenic lines were green under excitation light. Three week-old female C57BL/6 mice were purchased from CLEA Japan (Tokyo, Japan). All animals were maintained and used in accordance with institutional guidelines under the approved protocols.

Bone marrow transplantation (BMT). About 12 h after sublethal irradiation (9 Gy), the recipient 3 or 10 week-old female B6 mice received an injection of 1×10^7 BM cells from GFP Tg female mice via the tail vein. When mice were sacrificed to harvest the mammary gland, we confirmed the success of BMT by flow cytometric analysis of GFP expression using a FACSCalibur (Becton–Deckinson, Mountain View, CA) as previously described [28].

Hormonal treatment. Four weeks after BMT, hormone pellets purchased from Innovative Research of America (Sarasota, FL) were inserted subcutaneously into the backs of mice. These pellets contain 17- β estradiol (0.1 mg) and progesterone (32.5 mg), which are released continuously for 21 days. Mice were sacrificed 3 weeks later and mammary glands were analyzed.

Whole mammary gland transplantation (WMT). Whole mammary gland transplantation was carried out as previously described [31]. The entire fourth mammary gland with fat pad was removed from 3 week-old B6 female mice and was placed onto the abdominal wall of GFP Tg (B6) females the same age. After 4 weeks, a transplanted gland and an endogenous gland were analyzed. All surgical procedures were done under anesthesia with pentobarbital i.p.

Tissue processing and morphological analysis of the whole mammary gland. The fourth mammary glands were fixed, stained in carmine-alum solution, and mounted on slides as previously described [12,32]. After being photographed, mammary gland whole mount preparations were measured from the nipple area to the tips of the three longest ducts through the lymph node to determine ductal lengths (in mm). Numbers of branches represent the mean branching number along the three longest ducts from the nipple area to the migration front.

Histological, immunohistochemical, and immunofluorescent microscopy. Prefixed, paraffin wax embedded mammary glands were sectioned at 5 μ m

and processed for H&E staining, immunohistochemistry, and immunofluorescent microscopy as previously described [28]. The primary antibody for immunohistochemical staining was rabbit polyclonal anti-GFP Ab (Molecular Probe, Eugene, OR). The primary antibodies used for immunofluorescent staining were: rabbit polyclonal anti-mouse Cytokeratin 5 (Covance, Princeton, NJ), Guinea pig polyclonal anti-cytokeratin 8/18 (Progen, Heidelberg, Germany), mouse monoclonal anti- α -SMA-Cy3 (1A4; Sigma), rabbit polyclonal anti-Factor VIII (Dako), and goat polyclonal anti-GFP Ab (Molecular Probes). Second antibodies for immunofluorescent microscopy were: Alexa Fluor 488 F (ab)² fragment of chicken anti-goat IgG (H + L), Alexa Fluor 546 F (ab)² fragment of goat anti-mouse IgG (H + L), Alexa Fluor 546 F (ab)² fragment of goat anti-Guinea pig IgG (H + L), and Alexa Fluor 546 F (ab)² fragment of goat anti-rabbit IgG (H + L) (Molecular Probes). Before mounting, all sections were stained with DRAQ5 (Alexis Biochemicals, Lausen, Switzerland) for the discrimination of nucleated cells. Confocal microscopy was performed using an LSM5 PASCAL (Carl Zeiss, Oberkochen, Germany). Confocal images were stored as digital files and viewed using Photoshop (Adobe, Mountain View, CA). We assessed negative control studies and obvious nonspecific signals could not be found in the current experiment.

Numbers of bone marrow-derived cells. After immunofluorescence staining, SMA/GFP double positive cells within the ductal structure were counted for the evaluation of myoepithelial cell. Periductal fibroblasts were assessed morphologically, and GFP-positive cells were counted. Both of BM-derived cells were counted in 20 fields (200 \times magnification) of each specimen by two investigators (TS and GI).

Preparation of single-stranded DNA probe and in situ hybridization for IGF-I. In situ hybridization using the digoxigenin (DIG)-labeled single-stranded DNA probe was carried out as previously described [33] as a template for RT-PCR of IGF-I. The cDNA fragment (270 bp) from the coding region of mouse IGF-I was amplified by RT-PCR with Thermo-script RT-PCR system (Invitrogen, Carlsbad, CA), using the following pairs of oligonucleotide primers:

Primer IGF-I (sense): 5'-TCGTCTTCACACCTCTTCTAC-3',
Primer IGF-I (antisense): 5'-CTTTGTAGGCTTCAGTGGG-3'.

In situ hybridization was performed with a DIG-labeled DNA probe Detection Kit (Dako, Carpinteria, CA) according to the manufacturer's protocol. Then, the sections were stained immunohistochemically with anti-GFP Ab, counterstained with nuclear fast red, mounted with Crystal/Mount (Biomedex, Foster City, CA), and analyzed under a light microscope.

Statistical analysis. Statistical analysis was performed using GraphPad Prism Ver.3.03 (GraphPad Software, San Diego, CA). All data were expressed as means \pm standard error (SE). Statistical evaluations were performed with a two-tailed unpaired *t* test. Differences at *P* < 0.05 were considered statistically significant.

Results

BM can serve as a source of myoepithelial cells and periductal fibroblasts

In this experiment, we irradiated 3 week-old recipient mice at 9 Gy for BMT. Since irradiation may induce tissue injury, possibly influencing the mammary gland development, we first evaluated the effect of irradiation on the mammary gland morphology. Morphological examination of whole mount preparations with carmine-alum staining revealed both ductal length and the number of ductal branches to be similar in mice with and without BMT at each week, and no significant differences were observed (date not shown). Thus, mammary gland ductal outgrowth

was unaffected by BMT as the process of creating BM chimera mice.

Three week-old B6 mice were sublethally irradiated and then transplanted with 1×10^7 BM cells obtained from female GFP Tg (B6) and mammary glands were analyzed at 10 weeks. An antibody specific for GFP was used to identify cells of BM origin. Lymphocytes in mammary gland lymph node were positive for GFP (Fig. 1A) whereas no GFP-positive lymphocytes were detected in the mice reconstituted with BM cells from GFP^{-/-} mice (Fig. 1B). In the BM chimera mice, GFP-positive cells were scattered around the mammary ducts (Fig. 1C). Within the ducts, GFP-positive cells were located in the basal layer of ductal epithelial cells (Fig. 1D). Judging from morphology and position, we speculated that these GFP-positive cells were myoepithelial cells. Outside the ductal tree, spindle-

shaped cells within the periductal stroma (periductal fibroblast) were also GFP positive (Fig. 1E). No GFP-positive cells were detected in ducts reconstituted with BM cells from GFP^{-/-} mice (Fig. 1F).

We performed an immunofluorescence staining for markers of myoepithelial cell; Cytokeratin 5 (CK5), α -SMA, and luminal epithelial cell; Cytokeratin 8/18 (CK8/18) [34,35]. As shown in Fig. 2A and C, CK5/GFP and α -SMA/GFP double positive cells were scattered within ductal structure. We could not find obvious GFP/CK8/18 double positive cells (Fig. 2E). Therefore we concluded that these GFP-positive cells were myoepithelial cells. On the contrary, GFP-positive fibroblasts were recognized adjacent to the mammary epithelium within periductal stroma tissue (Fig. 2B and D). We could not find any Factor VIII/GFP double positive cells within periductal space (Fig. 2F). These

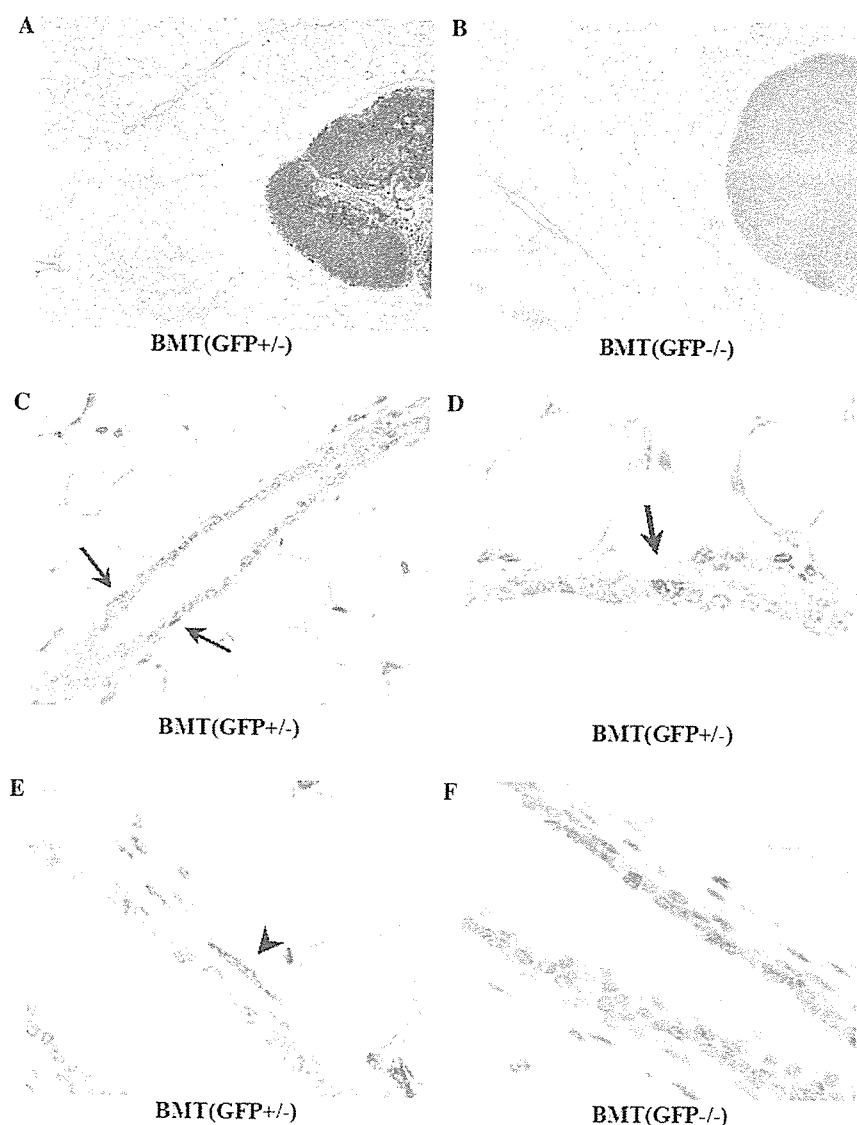


Fig. 1. Detection of BM-derived cells in BMT mice by immunohistochemical staining for GFP. (A) Lymph node of BMT^{GFP+/-} mice. Numerous lymphocytes were GFP positive. (B) Lymph node of BMT^{GFP-/-} mice. No lymphocytes were GFP positive. (C) Mammary gland of BMT^{GFP+/-} mice. Arrows indicate the GFP-positive cells in the mammary ductal component. (D) GFP-positive cell (arrow) was located in the basal layer of ductal epithelial cells. (E) GFP-positive spindle cell (arrowhead) was located in the connective tissue outside the ductal tree. (F) There were no GFP-positive cells in the mammary glands of BMT^{GFP-/-} mice.